

2023-02

Design and analysis of thyristor controlled series capacitor for enhancement of power transfer capability of a 230 Kv transmission system. Case study: (230 KV Transmission Line: - Legetafo to Debre Birhan)

Fitsum, Haile Meshe

<http://ir.bdu.edu.et/handle/123456789/15537>

Downloaded from DSpace Repository, DSpace Institution's institutional repository



BAHIR DAR UNIVERSITY

BAHIRDAR INSTITUTE OF TECHNOLOGY

SCHOOL OF RESEARCH AND POST GRADUATE STUDIES

FACULTY OF ELECTRICAL AND COMPUTER ENGINEERING

POWER SYSTEM ENGINEERING

MSc thesis on:

**Design and analysis of thyristor controlled series capacitor for
enhancement of power transfer capability of a 230 Kv transmission
system.**

**Case study: (230 KV Transmission Line: - Legetafo to Debre
Birhan)**

By:

Fitsum Haile Meshe

February 2023

Addis Abeba, Ethiopia



BAHIR DAR UNIVERSITY

BAHIR DAR INSTITUTE OF TECHNOLOGY

SCHOOL OF RESEARCH AND POST GRADUATE STUDIES

FACULTY OF ELECTRICAL AND COMPUTER ENGINEERING

POWER SYSTEM ENGINEERING

Design and analysis of thyristor controlled series capacitor for enhancement of power transfer capability of a 230 Kv transmission system.

Case study: (230 KV Transmission Line: - Legetafo to Debre Birhan)

BY

Fitsum Haile Meshe

A thesis submitted to the school of Research and Graduate Studies of Bahir Dar Institute of Technology, BDU in partial fulfillment of the requirements for the degree of master in the Power System Engineering in the Faculty of Electrical and Computer Engineering.

Advisor: Dr-Ing Belachew Bantyriga

February 2023
Addis Abeba, Ethiopia

DECLARATION

I, the undersigned, declare that this thesis comprises my own work. In compliance with internationally accepted practices, I have acknowledged and refereed all materials used in this work. I understand that non-adherence to the principles of academic honesty and integrity, misrepresentation/ fabrication of any idea/data/fact/source will constitute sufficient ground for disciplinary action by the university and can also evoke penal action from the sources which have not been properly cited or acknowledged

Name of the student: Fitsum Haile signature: _____

Date of Submission: _____

Place: Addis Abeba

© 2023

FITSUM HAILE MESHE

**Design and analysis of TCSC for enhancement of power transfer
capability of a 230 Kv transmission system.**

**Case study: (230 KV Transmission Line: - Legetafo to Debre
Birhan)**

All rights reserved

BAHIR DAR UNIVERSITY
BAHIR DAR INSTITUTE OF TECHNOLOGY
SCHOOL OF GRADUATE STUDIES
FACULTY OF ELECTRICAL AND COMPUTER ENGINEERING

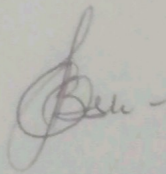
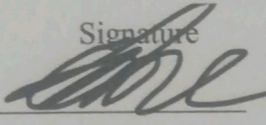
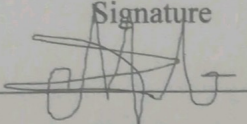

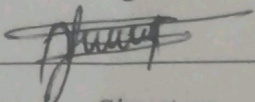
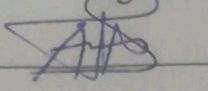
Approval of thesis for defense result

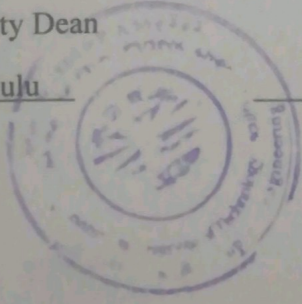
I hereby confirm that the changes required by the examiners have been carried out and incorporated in the final thesis.

Name of Student Fitsum Haile Signature _____ Date _____

As members of the board of examiners, we examined this thesis entitled "Design and analysis of thyristor controlled series capacitor for enhancement of power transfer capability of a 230 Kv transmission system" by Fitsum Haile. We hereby certify that the thesis is accepted for fulfilling the requirements for the award of the degree of Master of Science in "Power System Engineering".

Board of Examiners

Name of Advisor		Date
<u>Dr-Ing. Belachew Bantyrirga</u>	_____	<u>04.04.2023</u>
Name of External Examiner	Signature	Date
<u>Dr. Mengesha Mamo</u>		<u>March 27, 2023</u>
Name of Internal Examiner	Signature	Date
<u>Dr. Mezigebe Getnet</u>		<u>March, 28/2023</u>
Name of Chairperson	Signature	Date
<u>Dr. Tassew Tadiwose</u>		<u>March 31, 2023</u>
Name of Chair Holder	Signature	Date
<u>Mr. Yossef Berhan</u>		<u>APR 19 2023</u>
Name of Faculty Dean	Signature	Date
<u>Dr. Teketay Mulu</u>		<u>29/04/2023</u>




Mezigebe Getnet Yenealem
Assistant Professor (Ph.D.)
Post Graduate Coordinator

ACKNOWLEDGMENT

First and foremost, I'd like to express my gratitude to the Almighty God for his provision of grace to complete the entire work. Next, I'd like to thank and appreciate my advisor, Dr. Ing Belachew Bantyriga, for his advice and encouragement. My heartfelt thanks go to the Debre Birhan substation and EEU employees who helped me obtain the tools and data I needed for my research. Most importantly, I'd like to express my gratitude to my parents and friends for their support. I could not have finished the dissertation on time without their moral support.

ABSTRACT

Industry growth, increased power consumption, the installation of new feeders, and the extension of existing feeder lines have all contributed to an extraordinary increase in electrical energy demand at the Debre Birhan substation. The transmission line from Legetafo to Debre Birhan has a primary voltage of 230 kV and a current of 800 A. The transmission line's rating is around 184 MVA. Over the last year, the transmission line from Legetafo to Debre Birhan has had an average peak line load of 159.4 MW. There are several methods for increasing the transmission line's power transfer capacity. TCSC is the first among them. The Thyristor-Controlled Series Capacitor (TCSC) is a series compensator that is used in transmission lines to control the active power flow, increase net transferable power, reduce losses, and Instead of building new transmission lines, lower costs. In this thesis, the design and analysis of TCSC have been implemented and tested to increase the net transferable power. This work was done on a 230 KV double-circuit transmission line from Legetafo to Debre Birhan. The degree of series compensation is typically 30 % to 70%, and in this thesis, 70% of the line reactance is chosen for compensation. A separate fuzzy logic controller is used in each operating mode to control the firing angle of the TCSC. The TCSC's analysis and design were based on two scenarios. The first scenario involves placing TCSC at the sending end of the transmission line, while the second scenario involves placing TCSC at the receiving end of the transmission line. The TCSC capacitive modes are performed in both scenarios. When the TCSC is placed at the transmission line's sending end in capacitive mode, the active power flow increases from 140 MW to 180 MW, while the reactive power flow decreases from 74 MVAr to 20 MVAr. The total apparent power is 181 MVA. When the TCSC is placed at the receiving end of the transmission line in capacitive mode, the active power flow increases from 140 MW to 200 MW, while the reactive components fall from 74 MVAr to 10 MVAr, resulting in a total apparent power of 200.25 MVA. The results are better when TCSC is placed at the receiving end of the transmission line. The overall cost, including the installation cost of TCSC and the cost of the TCSC devices, is 76,294,400 ETB. The net annual return of the devices after installation is 466,207,200 ETB. The payback period of the devices is 2 years.

Keywords: Thyristor Controlled Series Capacitor, Power Flow, ANN, Fuzzy Logic Controller, MATLAB/SIMULINK

TABLE OF CONTENTS

DECLARATION	ii
ACKNOWLEDGMENT.....	v
ABSTRACT.....	vi
ABBREVIATIONS	xi
LIST OF TABLES	xiii
LIST OF FIGURES	xiv
CHAPTER ONE	1
1 INTRODUCTION	1
1.1 Background	1
1.2 Statement of problem	3
1.3 Objective	4
1.3.1 General objectives.....	4
1.3.2 Specific objectives	4
1.4 Significance of the study.....	4
1.5 Scope of the study	4
1.6 Methodology	4
1.7 Organization of the thesis.....	5
CHAPTER TWO	6
2 Literature Review.....	6
CHAPTER THREE	14
3 Theoretical Background.....	14
3.1 Load forecasting.....	14
3.1.1 Load forecasting classification	14
3.1.2 Factors consider in load forecasting	14
3.1.3 Load forecasting methods	14

3.2	Neural Network or Artificial Neural Network	15
3.2.1	Application area of neural network.....	16
3.2.2	The basic structure of ANN	17
3.2.3	ANN architecture	18
3.2.4	Learning Method.....	19
3.2.5	Workflow of ANN	21
3.3	FACTS Background.....	22
3.4	Types of FACTS Controller.....	24
3.5	Basic Principle and Mode of TCSC Operation	25
3.5.1	Blocked Thyristor Mode	26
3.5.2	Bypassed Thyristor Mode	27
3.5.3	Partially Conducting Thyristor or Vernier Mode.....	27
3.6	TCSC Layout and Protection	33
3.7	TCSC Capability Characteristics	35
3.8	TCSC Losses	35
	CHAPTER FOUR.....	36
4	Methodology (materials and methods)	36
4.1	Data Collection and analysis	36
4.2	Software used for modeling.	40
4.3	Model of the System without TCSC	41
	CHAPTER FIVE	42
5	Result and Discussion	42
5.1	Forecasting Future Load Demand through ANN	42
5.2	Simulink Model of TCSC for 230 KV Transmission Line	45
5.3	TCSC Placement and Sizing	46
5.3.1	Sizing of TCSC	46

5.3.2	TCSC Placement.....	47
5.4	Controller System.....	48
5.4.1	PI Controller.....	49
5.4.2	Fuzzy Logic Controller.....	50
5.5	Firing unit.....	53
5.6	Simulation Results and Discussion	54
	Case 1: Installing TCSC with 70 % compensation at the transmission line-sending end.....	55
	Case 2: Installing TCSC with 70 percent compensation at the transmission line receiving end.....	57
5.7	Cost-Benefit Analysis of TCSC	58
5.7.1	Cost of TCSC.....	58
5.7.2	Benefit of TCSC	59
5.7.3	Payback Period.....	61
CHAPTER SIX.....		62
6	CONCLUSION AND RECOMMENDATION.....	62
6.1	CONCLUSION	62
6.2	RECOMMENDATION	63
6.3	Future work	63
REFERENCES		64
APPENDIX.....		69
	APPENDIX A: Matlab Code For Medium Transmission Line Parameter.....	69
	APPENDIX B: Demand Forecasting Matlab Program.....	71
	APPENDIX C: The Ethiopian Electric Utility Energy Tariff	72
	APPENDIX D: Debre Birhan Substation Voltage Profile.....	72
	APPENDIX E: Debre Birhan Substation Receiving End Active Power (MW)	74

APPENDIX F: Debre Birhan Substation Receiving End Reactive Power (MVAR)
.....75

Appendix G: Debre Birhan Substation Receiving End Power Factor77

ABBREVIATIONS

ANN:	Artificial Neural Network
ASMO:	Ageist Spider Monkey Optimization
CA:	Constant angle
CB:	Circuit breaker
CC:	Constant current
CP:	Constant power
CPF:	Continuation Power Flow
EA:	Evolutionary Algorithms
EEP:	Ethiopian Electric Power
EPRI:	Electric Power Research Institute
FACTS:	Flexible AC Transmission System
FC:	Fixed capacitor
GDP:	Gross Domestic Product
GERD:	Great Ethiopian Renaissance Dam
GTO:	Gate Turn off
IEEE:	Institute of Electrical and Electronics Engineers
IGBT:	Insulated Gate Bipolar Transistors
IGCT:	Insulated Gate Commutated Thyristors
LC:	Inductor capacitor
LTLF:	Long-Term Load Forecast
MOV:	Metal Oxide Varistor
MTLF:	Mid-Term Load Forecast
NN:	Neural Networks

PAR: Phase Angle Regulator

PB: Push Button

PID: Proportional Integral Derivative

PI: Proportional Integral

PL: Peak Load

SCADA: Supervisory Control and Data Acquisition

SSSC: Static Synchronous Series Compensator

STATCOM: Static Synchronous Compensator

STLF: Short Term Load Forecasting

SVC: Static VAR Compensator

TCPST: Thyristor-controlled phase-shifting transformers

TCR: Thyristor-controlled Reactor

TCSC: Thyristor Controlled Series Capacitor

TL: Transmission Line

TSC: Thyristor-Switched Capacitor

TSR: Thyristor-Switched Reactor

TTC: Total Transfer Capability

UHSC: Ultra-High-Speed Contact

UPFC: Unified Power Flow Controller

LIST OF TABLES

TABLE 2-1 SUMMARY OF THE LITERATURE REVIEW.....	13
TABLE 4-1 INPUT LAYERS DATA.....	36
TABLE 4-2 TRANSMISSION LINE DATA.....	38
TABLE 5-1 INPUT-OUTPUT TRAINING PATTERN.....	42
TABLE 5-2 INPUT-OUTPUT TESTING PATTERN.....	43
TABLE 5-3 PEAK LOAD FORECASTED.....	44
TABLE 5-4 SIMULATION PARAMETERS.....	47

LIST OF FIGURES

FIGURE 3-1 BASIC STRUCTURE OF THE ARTIFICIAL NEURAL NETWORK	18
FIGURE 3-2 ANN FEEDFORWARD [26]	19
FIGURE 3-3 ANN FEEDBACK WARD[26]	19
FIGURE 3-4 BLOCK DIAGRAM OF A SUPERVISED-LEARNING METHOD[25]	20
FIGURE 3-5 BLOCK DIAGRAM OF AN UNSUPERVISED-LEARNING METHOD [25].....	21
FIGURE 3-6 OVERVIEW OF FACTS DEVICES	23
FIGURE 3-7 INDUCTOR CONNECTED IN SHUNT WITH AN FC	25
FIGURE 3-8 BLOCKED THYRISTOR MODE.....	26
FIGURE 3-9 BYPASSED THYRISTOR MODE	27
FIGURE 3-10 PARTIALLY CONDUCTING THYRISTOR CAPACITIVE VERNIER	28
FIGURE 3-11 PARTIALLY CONDUCTING THYRISTOR INDUCTIVE VERNIE	28
FIGURE 3-12 SIMPLIFIED TCSC CIRCUIT.....	29
FIGURE 3-13 IMPEDANCE VS FIRING ANGLE CHARACTERISTICS CURVE	32
FIGURE 3-14 FACTCS MODULE A) A BASIC MODULE B) A PRACTICAL MODULE [31].....	33
FIGURE 3-15 TYPICAL TCSC SYSTEM [6]	34
FIGURE 4-1 SINGLE LINE DIAGRAM OF TRANSMISSION LINE.....	37
FIGURE 4-2 REPRESENTATION OF TWO-PORT NETWORK	37
FIGURE 4-3 SINGLE-LINE DIAGRAM OF DEBRE BIRHAN SUBSTATION.....	39
FIG 4-4 MODEL OF THE SYSTEM WITHOUT TCSC	41
FIGURE 5-1 TRAINING PATTERN VS ACTUAL OUTPUT	43
FIGURE 5-2 TESTING PATTERN VS ACTUAL OUTPUT	44
FIGURE 5-3 VALIDATION PERFORMANCE	44
FIGURE 5-4 REGRESSION PLOT	44
FIGURE 5-5 SIMULINK MODEL OF TRANSMISSION LINE WITH TCSC INSTALLED AT THE SENDING END.....	45
FIGURE 5-6 SIMULINK MODEL OF TRANSMISSION LINE WITH TCSC INSTALLED AT THE RECEIVING END.....	46

FIGURE 5-7 TCSC CONTROL SYSTEM DIAGRAM.....	49
FIGURE 5-8 PI CONTROLLER OF TCSC.....	49
FIGURE 5-9 FUZZY LOGIC CONTROLLER OF TCSC	50
FIGURE 5-10 CAPACITIVE MODE MAMDANI FUZZY INTERFACE	51
FIGURE 5-11 CAPACITIVE MODE INPUT MEMBERSHIP FUNCTION	51
FIGURE 5-12 CAPACITIVE MODE OUTPUT MEMBERSHIP FUNCTION	52
FIGURE 5-13 INDUCTIVE MODE MAMDANI FUZZY INTERFACE	52
FIGURE 5-14 INDUCTIVE MODE INPUT MEMBERSHIP FUNCTION	53
FIGURE 5-15 INDUCTIVE MODE OUTPUT MEMBERSHIP FUNCTION	53
FIGURE 5-16 SIMULINK MODEL OF A FIRING UNIT	54
FIGURE 5-17 SENDING END ACTIVE POWER FLOW ON THE CAPACITIVE MODE OF OPERATION	55
FIGURE 5-18 SENDING END ACTIVE POWER VS REACTIVE POWER ON CAPACITIVE MODE.....	56
FIGURE 5-19 RECEIVING END ACTIVE POWER FLOW ON THE CAPACITIVE MODE OF OPERATION	57

CHAPTER ONE

1 INTRODUCTION

1.1 Background

The rapid increase in electrical energy consumption, combined with the demand for low-cost energy, has gradually resulted in the development of generation sites located far from load centers. Remote generating stations, in particular, include hydroelectric stations, which exploit sites with higher heads and significant water flows; fossil fuel stations near coal mines; site-bound geothermal and tidal-power plants; and, occasionally, nuclear power plants purposefully built far from urban centers. Transmission lines are required to connect generation sites to load centers when generating bulk power in remote locations. Furthermore, to improve system reliability, multiple lines connecting load centers to multiple sources, interconnecting neighboring utilities, and constructing the necessary levels of redundancy have gradually led to the evolution of complex interconnected electrical transmission networks. These networks can now be found on all continents[1].

In recent years, the high cost of building new transmission lines, combined with the difficulty of obtaining new transmission corridors, has prompted a search for ways to increase the transmission capacity of existing lines. The transmission line's series compensation is modeled to improve power flow at the receiving end. Capacitors are used in series compensation to compensate for the inductive reactance of long lines. It is a highly effective and cost-effective method of increasing power transfer capacity for both new and existing lines. Series compensation improves voltage stability and increases power transfer capability by raising the transient stability limit[2].

The introduction of the FACTS concept and components has resulted in new methods of increasing the existing power system's stability limit. This is accomplished by incorporating modern controllable components into the grid. The Thyristor controlled series capacitor, which is the focus of this thesis, is an example of such a device.

FACTS has two primary goals [3]:

- To increase the capability of transmission lines.
- Control power flow over a transmission line electronically and statically, without the need for operator intervention, mechanical manipulations, or conventional breakers switching.

Thyristor controlled series compensation (TCSC): A TCSC configuration consists of controlled reactors connected in series with a section of the capacitor bank. The combination enables smooth control of capacitive reactance over a wide frequency range. Each phase's capacitor bank is mounted on a platform for complete ground insulation. The thyristor valve is made up of a series of high-power Thyristors. The inductor is off air-core construction. To prevent overvoltage, a metal oxide varistor (MOV) is connected across the capacitor [4].

1.2 Statement of problem

The transmission line from Legetafo to Debre Birhan has a primary voltage of 230 kV and a current of 800 A. The transmission line's rating is around 184 MVA.

Over the last year, the average active power of the line has been approximately 140 MW, the average reactive power has been around 74 MVar, and the average power factor of the transmission line has been around 0.8 lagging power factor. Over the last year, the transmission line from Legetafo to Debre Birhan has had an average peak line load of 159.4 MW.

The average rate of demand growth is rapid. The expansion of industry, the construction of new feeders, and the expansion of existing feeders have all contributed to an enormous increase in electrical energy demand in the Debre Birhan.

It is not only costly but also time-consuming to build a new power transmission line system, but it is also necessary to make effective use of the existing transmission line. On the other hand, overall power demand has increased year after year, contributing to a shortage of transmission capacity that can lead to power grid failure. As a result, there is a need to investigate various options for increasing the power transfer capacity of transmission lines. By improving this capability, the existing transmission line will become more efficient and easier to control the variables based on demand. In general, the power flow equation is $P = (V_s V_r / X) \sin \sigma$, where V_s represents the sending end voltage, V_r represents the receiving end voltage, and X represents the series reactance. If we change the series reactance X , we can increase or decrease the active power flow on the line. In practice, fixed capacitive compensation is used to reduce net series inductive reactance X , thereby increasing power flow on the transmission line. A sub-synchronous resonance problem exists with fixed capacitive compensation. This problem can be solved by using a Thyristor-controlled series capacitor, which is a versatile FACTS device.

For this proposed study, the research questions are as follows:

- Series compensation device (TCSC) should be recommendable?
- In which place (TCSC at the sending end or receiving end of the transmission line) is efficient?

1.3 Objective

1.3.1 General objectives

The study's main goal is to increase the transmission system's power handling capacity via a Thyristor-controlled series capacitor.

1.3.2 Specific objectives

- i. To analyze the current line loading.
- ii. To design and model a TCSC for capacitive mode of operation.
- iii. To determine the optimal TCSC placement and size.
- iv. To create a Fuzzy Logic Controller to control the firing angle.
- v. To examine the cost-benefit analysis of TCSC.

1.4 Significance of the study

There are two options for increasing the capacity of the transmission line (TL). The first is to build a new transmission line, and the second is to expand the existing transmission system's power transfer capacity.

Improving transmission line power handling capacity has several advantages when the thyristor-controlled series capacitor (TCSC) is optimally positioned. Increased net transferable power, lower losses, higher voltage reliability, and Instead of building new transmission lines, lower costs.

1.5 Scope of the study

The installation of TCSC in the transmission system increases the transmission system's power handling capacity. The study's goal is to improve the transmission line's power transfer capacity. The goals of this project are to simulate the proposed system using Matlab simulation software and to analyze the system performance enhancement before and after compensating with a thyristor-controlled series capacitor.

1.6 Methodology

- Literature Review: Review and read articles, books, and other relevant documents.

- Gathering the relevant data from Ethiopian Electric Power Corporation: line data, bus data, network base voltage, conductor size, impedance definitions, active power, reactive power, swing angle, lengths, previous load data, and so on.
- Forecasting load: forecasting is the first and primary step in planning the future requirements of the transmission system in an electric grid, forecasting is done through an Artificial neural network
- Data analysis: interpretation of the data like line data, bus data, network base voltage, impedance definitions, active power, reactive power, swing angle, lengths, previous load data, and so on.
- System modeling and result analysis: modeling transmission lines with and without TCSC.
- Conclusion and discussing
 - The final thesis result will be discussed and concluded.

1.7 Organization of the thesis

The thesis is divided into six chapters, which are summarized below.

Chapter 1, introduction and the transmission line problems are observed In addition, the overall objectives, scopes, and methods used to achieve the main goal have been briefly summarized.

Chapter 2 provides a summary of extensive literature reviews.

Chapter 3: All the theoretical background information has been provided. FACTS background, basic principles and mode of TCSC operation, TCSC layout and protection, TCSC capability characteristics, load forecasting, and artificial neural network are all discussed.

In Chapter 4, this work's general methodology was stated.

In Chapter 5, the outcome and discussion were discussed.

Chapter 6 This concludes the work completed and the outcomes obtained. Future work recommendations were also presented.

CHAPTER TWO

2 Literature Review

In 2017, Gebrmichael Gebre study the relevance of TCSC, or Series Compensation, for improving transmission line usage at Dedesa substation of a 500kV transmission system stretching from GERD to Holeta substation, and designed TCSC as a good alternative for power oscillation dampening and SSR mitigation. The DigSILENT software is used to implement the system. And improves the system's steady and dynamic stability of power, voltage, and current [5].

In 2019 Abebaw Yalew studied the impact of the SVC in the HOLETA 500 /400kV substation on voltage stability and power transfer improvement. At the HOLETA 500/400 kV substation, three SVCs with a total capacity of 900 Mvar are used. They are linked to the 400 kV AC system by 400/33 kV coupling transformers. The study also examined the impact of installing SVCs at DEESA or GERD substations on voltage stability and transferred power. The system is simulated in this study using the MATLAB 2017a /Simulink environment [6].

In 2019 Girma Zeleke studied Long-term load forecasting for the entire country is performed using an Artificial Neural Network (ANN), and transmission system expansion planning to meet the country's future load demand is investigated using the highly interactive MATLAB and ETAP 16 software. The performance of Ethiopian Electric Power's (EEP) existing transmission system for the central and southern regions is investigated using load flow analysis to identify and locate overloading problems in the system. A method for selecting the best possible transmission system expansion plan is presented [7].

In 2020 Ananda M. H, M. R. Shivakumar proposed series capacitors are used in higher voltage cables, so power can be shifted from overloaded lines, increasing the utilization of the existing line while also enhancing the power system's performance. The goal of this research is to demonstrate effective line network usage for maximum power flow across the targeted line with series capacitor compensation using a three-line meshed power system network with various thermal line limits. Simulations using the Power World simulator show that adding a series capacitor boosts power transfer over the line up to its thermal limit[8].

In 2019 Gang Wu, Baodong Wang, Shufeng Liu, and Hao Wan study the idea of series compensation technology in distribution networks, as well as the topology structure and application benefits of a fixed series capacitance compensation device. The capacity selection of the series compensation device is demonstrated using the design of a 35kV series compensation device in Linlang station as an example. The voltage, line loss, and voltage fluctuation rate are examined with and without the use of a series compensation device. The economic advantages of the series of compensating devices are also discussed. The engineering example also demonstrates that series compensation technology is an excellent approach for increasing line transmission power, improving system stability, and improving line voltage quality. As a result, series compensation technology has a lot of advantages in the field[9].

In 2020 Valery Golov, Andrew Kalutskov, and Dmitry Kormilitsyn study the effects of series compensation devices installed on 220 kV lines on system stability and current load. And also recommended that the aperiodic steady-state stability of an electric power system with 220 kV power lines be investigated, as well as the issues of improving the transmission capacity of the power transmission line[10].

In 2017 Nirav Patel, Study simulation and hardware of single-phase TCSC, the value of resistor of a constructed air-core winding and inductor was identified by the least square method. The laboratory model for the single-phase TCSC system is built with Arduino Uno and tested by loading the pulse generation program into Arduino Uno. The Pi transmission line was designed and built for single-phase voltage levels. The simulation of a single-phase TCSC was created using the MATLAB R2014a software. Finally, validation was performed by comparing simulation and hardware results[11].

In 2020 Pradeep Singh; Rajive Tiwari; Venu Sangwan; Abhilash Kumar Gupta proposed an Ageist Spider Monkey Optimization (ASMO) algorithm and a fuzzy logic-based approach to seeking the optimal locations and sizing of Thyristor-controlled series capacitors (TCSC) and Thyristor-controlled phase-shifting transformers (TCPST) in the power sector to improve voltage stability margins and reduce active and reactive power losses. The proposed algorithm is also used to compare the attributes of the aforementioned FACTS devices. A quarter cosine fuzzy membership function can determine the membership values of variables defined in various objectives. The

proposed method's application was investigated on standard IEEE 30 and 118-bus systems [12].

In 2009 C. Bulac, C. Diaconu, M. Eremia, B. Otomega, I. Pop, L. Toma, and I. Tristiu presents the findings of a feasibility study for installing FACTS devices in the Romanian power grid's south-eastern region (Dobrogea - a peninsular area), to increase the grid's overall transfer capacity. On the one hand, this study assumed a planned increase in generated power in the area, owing primarily to two new units at the Cernavod nuclear power plant (1400 MW installed power) and wind generation with an estimated installed power of over 1600 MW. The scenarios, on the other hand, took into account the transmission network's current topology as well as future developments[13].

In 2010 Vjollca Komoni, Isuf Krasniqi , Gazmend Kabashi , and Avni Alidemaj discusses how FACTS controllers can be used to increase power system capability and control line power flow in power systems. FACTS improve power system performance, improve supply quality, and make the best use of existing resources. Various FACTS controller devices, particularly SVC and STATCOM, allow load flow on parallel circuits to be optimized and controlled while minimizing power wheeling, maximizing line utilization, and minimizing overall system losses. The goals were to determine the power transfer capability of the power system, identify ways to increase the transfer limit, and test the potential application of FACTS devices. The analytical approach, computational tools, and simulation models are all described in the paper [14].

In 2015 S Bagchi, R Bhaduri, P N Das, and S Banerjee provides insight for improving power transfer capability in long transmission lines by analyzing and comparing several FACTS devices such as Static Var Compensator (SVC), Static Synchronous Compensator (STATCOM), and Unified Power Flow Controller (UPFC). These devices have been used in a variety of locations, including the transmission line's sending, middle, and receiving ends. Each model's appropriate location and performance have been evaluated. First, real and reactive power profiles for an uncompensated system were investigated, and results were obtained. The results are then compared to the results obtained after compensating the system with the aforementioned FACTS devices. Overall, the analysis shows that when SVC is

connected in the middle of the transmission line, more power (87.24 %) is transferred. All simulations have been done in MATLAB/SIMULINK [15].

In 2017 Shaswat Chirantan, Ramakanta Jena, Dr.S.C.Swain, and Dr.P.C.Panda studied on Comparative analysis of STATCOM And TCSC FACTS controllers for power profile enhancement in a long transmission line. a shunt type controller, STATCOM (Static Synchronous Compensator), and a series type controller, TCSC (Thyristor Controlled Series Capacitor), have been considered in this paper. The variation of real and reactive power (power profile) caused by the introduction of STATCOM & TCSC at various locations along a long transmission line was investigated in this study. All of these analyses are carried out by the STATCOM and TCSC Matlab/Simulink models[16].

In 2016 Nikita M. Malwar, S. R. Gaigowal, and Abhijit A. Dutta investigates an SSSC control scheme to improve the dynamic performance of a transmission line. Flexible AC Transmission Systems (FACTS) devices are used to make the power system more advanced and controllable. The Static Synchronous Series Compensator (SSSC) is a series FACTS device that can provide controllable compensating voltage over a capacitive and inductive range while remaining independent of line current. The voltage source converter is coupled with a transformer that is connected in series with a transmission line in SSSC. It is validated by the results of MATLAB simulations of SSSC operation under various load conditions [17].

In 2016 Pooja Nagar, and S. C. Mittal presents the dynamic result of a static synchronous series compensator. To investigate the effect of this device in controlling the power flow through a transmission line, a voltage source inverter equipped with a dc source is used as an SSSC (static synchronous series compensator). This device not only acts as a reactive power compensator, but it can also supply and absorb active power from the transmission line. For both active and reactive power, the SSSC control system employs two closed loops. In addition to reactive power compensation, SSSC improves the voltage profile in the system. The results of simulations for various conditions are also described [18].

In 2016 O. Ziaee, and F. Choobineh presents the presence of a thyristor-controlled series capacitor (TCSC) device in a transmission network reduces network congestion and generation costs. They model the TCSC location-allocation problem as a mixed-

integer nonlinear program and propose a novel decomposition procedure for determining the optimal location and size of TCSCs in a network. The uncertainty of the load, the AC characteristic of transmission lines, and the nonlinear cost of TCSCs are explicitly considered. The procedure's results on the IEEE 118-bus test system are reported, and insights into the TCSC location-allocation problem are provided [19].

In 2019 Handika Putra, and Irfan Joyokusumo propose a study to examine the Total Transfer Capability (TTC) caused by the installation of a Unified Power Flow Controller (UPFC). The simulation is carried out using the Continuation Power Flow (CPF) method on the IEEE-14 Bus System. The simulation results show that UPFC placement based on bus voltage stability on the PV-curve can be used to increase the value of transmission line TTC. As a result, when the system is fully loaded, the UPFC is best located on the line that connects to the bus voltage that has the closest value to the maximum voltage drop constraint. As a result, the UPFC placements in scenarios 3 (3.3035 p.u.) and 4 (3.3017 p.u.) are the best places to increase the TTC value. This research is expected to be used as a justification for UPFC placement in the real transmission lines system [20].

The following is a summary of the literature review.

Authors name	Contribution/Finding	Limitation
Gebremichael Gebre, 2017	Analyze the importance of TCSC for transmission line utilization, a good alternative for power oscillation damping and SSR mitigation.	The scenario depends only on current transmission network topology and doesn't consider future developments
Abebaw Yalew, 2019	Show the improvements in voltage stability through SVC	Only normal and loading condition is checked not fault condition.
Girma Zeleke, 2019	Load term load is forecasted using ANN and analyzed in transmission system planning	The paper describes two forecasting methods, the Ethiopian electric power

	for Ethiopia's central and southern regions.	(EEP) and the EEP master plan (PB), but does not state their limitations.
Ananda M. H, M. R. Shivakumar, 2020	A three-line meshed power system network with different thermal line limits is considered to demonstrate effective line network utilization for maximum power flow through the intended line with series capacitor compensation.	The research is constrained only by the thermal limit, but the power system loading capability is constrained by operating constraints and voltage constraints.
Valery Golov, Andrew Kalutskov, and Dmitry Kormilitsyn, 2020	Investigate the effects of series compensation devices installed on 220 kV lines on system stability and the current load of system elements.	Effect of series compensation tested only on Current load of the system elements
Nirav Patel, 2017)	The laboratory model for the single-phase TCSC system is implemented using Arduino Uno and it is significance on active power and transmission line losses are identified.	The simulation test is done for small voltage only.
Pradeep Singh, Rajive Tiwari, and Venu Sangwan, 2020	Reduce active and reactive power loss, and improve voltage stability margin by using ageist spider monkey optimization algorithm and fuzzy logic-based approach	The algorithm is done individually, it's better to show a hybrid of the two algorithm
Bulac, C. Diaconu, M. Eremia, B.	Feasibility study for installing SVC devices in the	There are many techniques for the Optimal placement

Otomega, I. Pop, L. Toma, and I. Tristiu. 2009	southeastern part of the Romanian power grid for the transfer capacity to the rest of the grid.	and sizing of SVC, none of the algorithms is mentioned.
Vjollca Komoni, Isuf Krasniqi , Gazmend Kabashi , and Avni Alidema, 2010	Using SVC and STATCOM presents an increased power system capability and controlling line power flow in the power system	The device's best suitable location is not mentioned.
S Bagchi, R Bhaduri, P N Das, and S Banerjee, 2015	This paper gives insight into the improvement of power transfer capability by analyzing and comparing several FACTS devices such as Static Var Compensator (SVC), Static Synchronous Compensator (STATCOM) and Unified Power Flow Controller (UPFC) in long transmission line	The paper compare FACTS devices based on power transfer capability only, voltage stability is also a major one
Shaswat Chirantan, Ramakanta Jena, Dr.S.C.Swain, and Dr.P.C.Panda, 2017	The variation of reactive and real power by the installation of TCSC & STATCOM at various location in a long transmission line have been investigated	The investigation is considered only on power profile (Active and Reactive power)
Nikita M. Malwar, S. R. Gaigowal, and Abhijit A, 2016	Investigate the SSSC control scheme to improve the dynamic performance of transmission lines.	The paper does not discuss the best suitable location and sizing for SSSC, nor does it discuss voltage

		profile improvements in the system.
Pooja Nagar, and S. C, 2016	A voltage source inverter with a dc source is used by an SSSC to investigate its effect on controlling the power flow through a transmission line.	There are many techniques for optimum SSSC placement and sizing, but none of the algorithms are mentioned.
O. Ziace, and F. Choobineh, 2016	Using a mixed-integer nonlinear program and a novel decomposition procedure, determine the size and optimal location of the TCSC on the IEEE 118 bus.	The engineering effectiveness of the TCSC placement and size is evaluated, but different loading conditions are not taken into account.
Handika Putra, and Irfan Joyokusumo, 2019	By implementing the Continuation Power Flow (CPF) method on IEEE-14 Bus System, to decide the best location of UPFC to increase the total transfer capability	The placement analogy is considered only bus bar voltage stability

Table 2-1 Summary of the literature review

CHAPTER THREE

3 Theoretical Background

3.1 Load forecasting

3.1.1 Load forecasting classification

Load forecasts can be classified into three types based on their time horizon: short term, midterm, and long term[21].

- Short-term load forecasting (STLF): It is critical for various operational functions such as economic dispatch, unit commitment, real-time control, and energy transfer schedule to collect data over time intervals ranging from an hour to a week.
- Mid-term load forecast (MTLF): MTLF has a period ranging from a month to a year or two. The goal of MTLF is to balance generation and demand through Load dispatch, price settlement, maintenance schedule, and coordination
- Long-term load forecast (LTLF): The period of LTLF is a few years (>1 year) to 10–20 years ahead. LTLF aims at system expansion planning, i.e. distribution, generation, and transmission. It also has an impact on the purchase of new generating units in some cases.

3.1.2 Factors consider in load forecasting

Several factors should be considered for STLF, such as time factors, weather data, and possible customer classes. It also takes into account the number of customers in different categories and their characteristics [21].

The load pattern is influenced by three major time factors. These are seasonal effects, weekly/daily cycles, and holidays, all of which have an impact on load patterns.

3.1.3 Load forecasting methods

There are two basic types of Load forecasting methods based on their mathematical level of analysis [22].

- quantitative methods
- qualitative methods.

Planners primarily use qualitative forecasting methods to produce an accurate forecast. Under these categories, load forecasting can be classified into three major groups [22][23].

- Traditional Technique

Traditional forecasting is one of the critical topics for determining future load demands for infrastructure development, development trends, and the country's development catalog, among other things. These estimates were initially made using traditional/conventional mathematical techniques. These techniques have been improved for use in a variety of forecasting studies as a result of the development of progressive tools.

This technique is classified as the Regression Method, Multiple Regression Method, and Exponential Smoothing Method.

- Modified-Traditional Technique

Traditional forecasting techniques are improved so that the forecasting model's constraints auto-update in response to changing environmental conditions. Traditional techniques that have been improved include adaptive load forecasting, time series analysis, and support vector machine-based techniques.

- Soft Computing Technique.

The soft-computing technique has proven to be effective. It has seen widespread use in recent years. Soft computing is a developed approach that corresponds to the exceptional ability of the human mind to learn and reason in an unpredictable and inaccurate environment. It is evolving as a tool to aid computer-based intelligent systems in replicating the human mind's ability to use inexact rather than precise modes of reasoning. Soft computing is an order that includes neural networks(NNs), fuzzy logic, evolutionary algorithms(EAz), and others.

3.2 Neural Network or Artificial Neural Network

A neural network is a network of interconnected basic processing elements, units, or nodes whose functionality is based on the animal neuron. The inter-unit connection

strengths, or weights, generated through a process of adaptation to, or learning from, a set of training patterns, store the network's processing ability [24].

Artificial neural networks are mathematical creations inspired by observations made in the study of biological systems, though they are only loosely based on biology. An artificial neural network can be thought of as a mapping from one space to another. This is similar to the concept of a mathematical function. A neural network's purpose is to map an input into the desired output. While artificial neural networks are patterned after the interconnections between neurons found in biological systems, they are no more related to real neurons than feathers are to modern airplanes [25].

ANN is based on the principle of largely interconnected simple elements performing network functions, which was inspired by the biological nervous system. No prior knowledge is assumed, but data, records, measurements, and observations are taken into account. ANN research is based on the concept of learning from data to mimic the biological capability of solving linear and nonlinear problems [26].

3.2.1 Application area of neural network

Neural networks are widely used to solve a variety of problems that are difficult for humans or traditional computational algorithms to solve. The famous 1988 DARPA neural network study provided a comprehensive list of neural network applications such as word recognizer, process monitor, adaptive channel equalizer, analysis system, sonar classifier, risk, and so on. A list of neural network applications is provided below to give you an idea of how versatile they can be. The list is only a sampling of the numerous application fields [26].

- Time series prediction
 - Weather forecast
 - Financial prediction
 - Load forecast
- Robotics
 - Robotic speech recognition
 - Motion planning
 - Robotic version
- Financial

- Market Forecasting
- Product development optimization
- Trading optimization
- Market analysis
- Investment analysis
- Image Processing
 - Handwritten character recognition
 - Image recognition
 - Face, facial expression recognition
 - Front/letter recognition
- Signal processing
 - Signal and object separation
 - Signal classification
 - Signal conditioning
 - Noise classification and reduction
 - Feature extraction
 - Data compression
- Speech processing
 - Speech coding
 - Speaker-dependent/independent speech recognition
 - Speaker identification

3.2.2 The basic structure of ANN

A biological neuronal network is made up of many interconnections between neurons. The strength of a neuron is derived from its collective behavior in a network in which all neurons are interconnected. It is assumed that approximately 10 billion neurons act collectively in a human brain via approximately 10^{14} interconnections. Similarly, ANN emerges from the interconnections of several unit neurons or nodes. The following layers of neurons are most commonly used in the artificial network [24]–[26].

- Input layer

The number of neurons in this layer corresponds to the number of neuronal network inputs. This layer is made up of passive nodes that do not participate in signal modification and instead simply transmit the signal to the next layer.

- Hidden layer

This layer contains an arbitrary number of layers and neurons. This layer's nodes are active because they participate in signal modification.

- Output layer

The number of neurons in the output layer corresponds to the number of neural network output values. This layer contains active nodes.

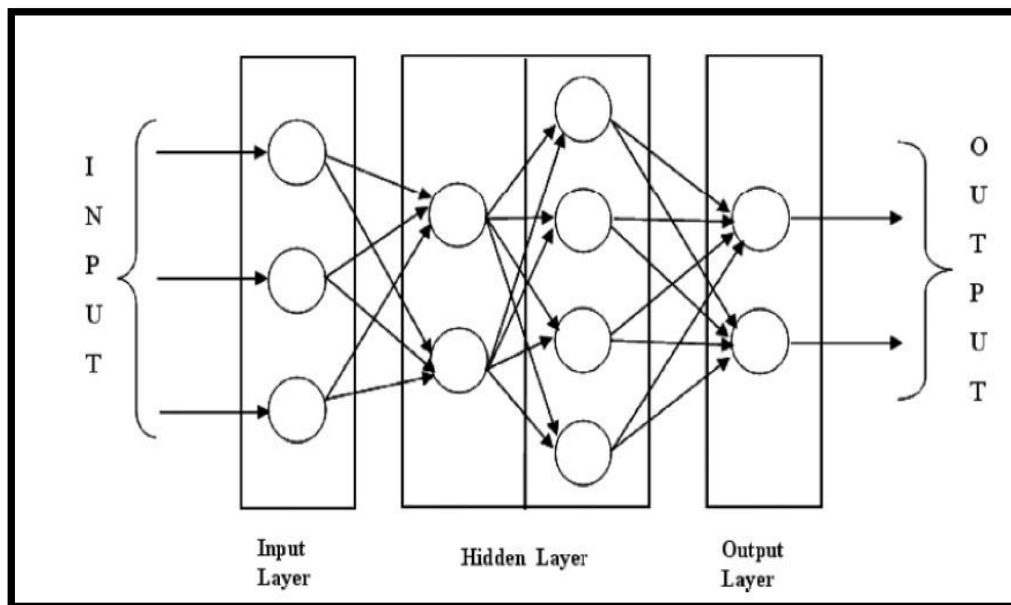


Figure 3-1 Basic Structure of the artificial neural network

3.2.3 ANN architecture

The term architecture refers to a network's connectivity. Different neuronal network types can be defined based on the type of interconnection of the neurons and the training algorithm used to fit the weights. These can be divided into two major categories.

- Feedforward

Where data flow is strictly fed forward from input to output units The data processing can span multiple layers of units, but no feedback connections, that is, connections extending from unit output to unit inputs in the same or previous layers, are present.

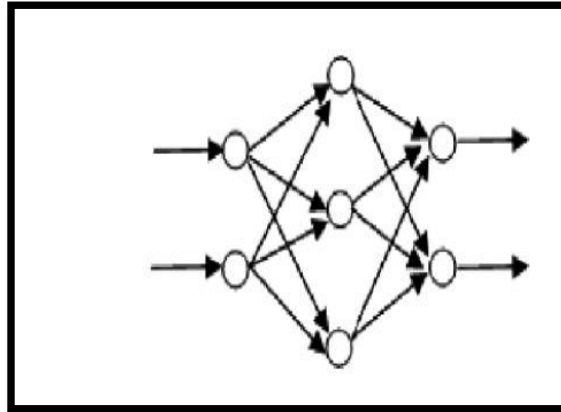


Figure 3-2 ANN Feedforward [26]

- Feed backward

The output of a neuron is either directly or indirectly fed back to its input via other linked neurons.

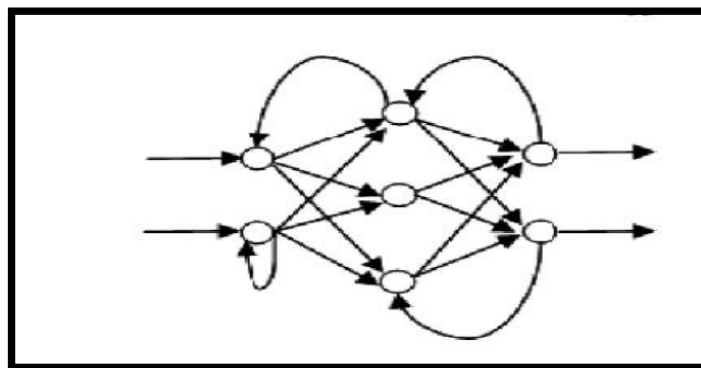


Figure 3-3 ANN Feedback ward[26]

3.2.4 Learning Method

A neural network must be configured in such a way that applying a set of inputs results in the desired set of outputs. There are several methods for determining the strength of the connections. One method is to explicitly set the weights based on prior knowledge.

Another method is to train the neural network by feeding it training patterns and allowing it to change its weights based on some learning rule [24]–[26].

- Supervised learning

A method of training a neural network by feeding it input and matching output patterns. These input/output pairs can be supplied by an external teacher or by the system that contains the network[27].

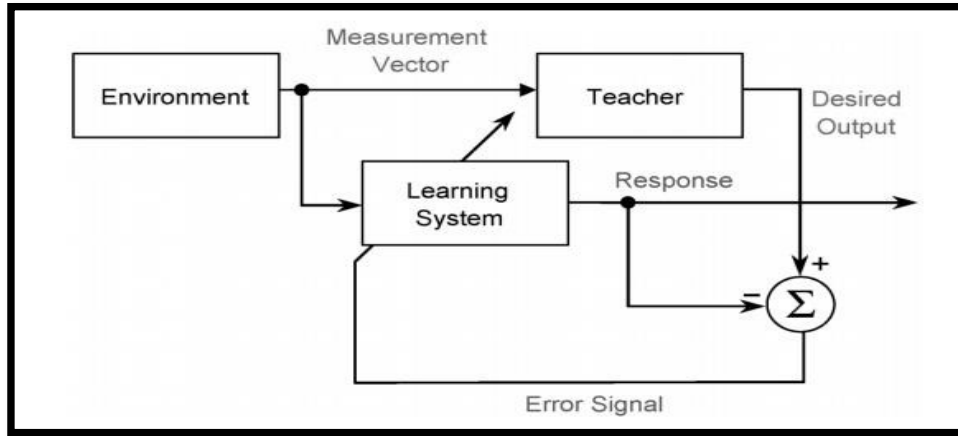


Figure 3-4 Block diagram of a supervised-learning method[25]

- Unsupervised learning

An output unit is trained to respond to pattern clusters in the input. The system is supposed to discover statistically significant features of the input population in this paradigm. In contrast to the supervised learning paradigm, there is no predefined set of categories into which the patterns must be classified; rather, the system must develop its representation of the input stimuli[27].

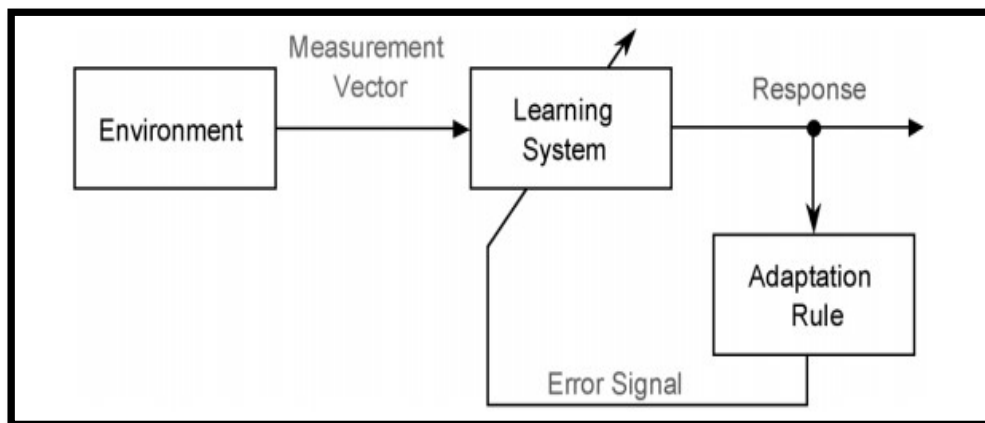


Figure 3-5 Block diagram of an unsupervised-learning method [25]

3.2.5 Workflow of ANN

There are seven primary steps in the neural network design process's workflow [28].

1. Collect data
2. Create the network — Create Neural Network Object
3. Configure the network — Configure Shallow Neural Network Inputs and Outputs
4. Initialize the weights and biases
5. Train the network — Neural Network Training Concepts
6. Validate the network
7. Use the network

Data collection in step 1 generally occurs outside the framework of Deep Learning Toolbox software, but it is discussed in general terms in Multilayer Shallow Neural Networks and Backpropagation Training.

The network object is used by the Neural Network Toolbox software to store all of the information that defines a neural network. This topic describes the fundamental components of a neural network and demonstrates how they are created and saved in the network object.

After constructing a neural network, it must be configured and trained. Configuration entails arranging the network in such a way that it is compatible with the problem at hand, as defined by sample data. After the network has been configured, the adjustable network parameters (known as weights and biases) must be tuned to optimize network performance. This process of fine-tuning is known as "network training." Example data must be provided to the network during configuration and training. All of this is also accomplished by using the ANN Toolbox's subsequent wizards in the MATLAB program

3.3 FACTS Background

FACTS is made up of many concepts that have been developed over many years of research and development. Nonetheless, FACTS, an integrated philosophy, was created in the 1980s at the Electric Power Research Institute (EPRI), the research arm of North American utilities (Hingorani and Gyugyi, 2000)[4].

Energy demand has risen in recent years. In this scenario, the project's key concerns are energy challenges, environmental concerns, land expansion onto neighboring properties, and the installation of new transmission lines. There have been a few ideas proposed in response to this circumstance to improve the power transfer capabilities and power quality of systems. Engineers have attempted to create a flexible device that will allow electricity networks to operate at their best.

Flexible AC Transmission Systems, or FACTS, has become a well-known word in recent years for increased controllability in power systems through the use of power electronic equipment. Several FACTS devices have been introduced around the world for diverse uses. Several new types of gadgets are currently being tested in the field. In research and literature, more notions of FACTS-device setups are considered[29].

FACTS is one facet of the power electronics revolution that is overtaking the electric energy industry. A variety of powerful semiconductor devices not only provide the advantages of high switching speed and reliability, but they also provide the chance to enhance the value of electric energy through a variety of new circuit concepts based on these power devices[1].

FACTS technology brings up new potential for regulating electricity and increasing the useful capacity of current lines as well as new and upgraded lines, which is particularly interesting and exciting for transmission planners. The ability to regulate current over a line at a minimal cost opens up a lot of options for upgrading old lines with larger conductors and using one of the FACTS Controllers to allow corresponding power to flow through such lines under normal and emergency conditions[1].

The taxonomy of 'dynamic' and static in terms of FACTS requires some clarification. The term 'dynamic' is used to describe the power electronics' capacity to manage FACTS devices quickly. This is one of the primary features that set it apart from other devices. The phrase "static" refers to devices that do not have any moving parts, such

as mechanical switches, that allow for dynamic controllability. As a result, most FACTS devices can be both static and dynamic[29].

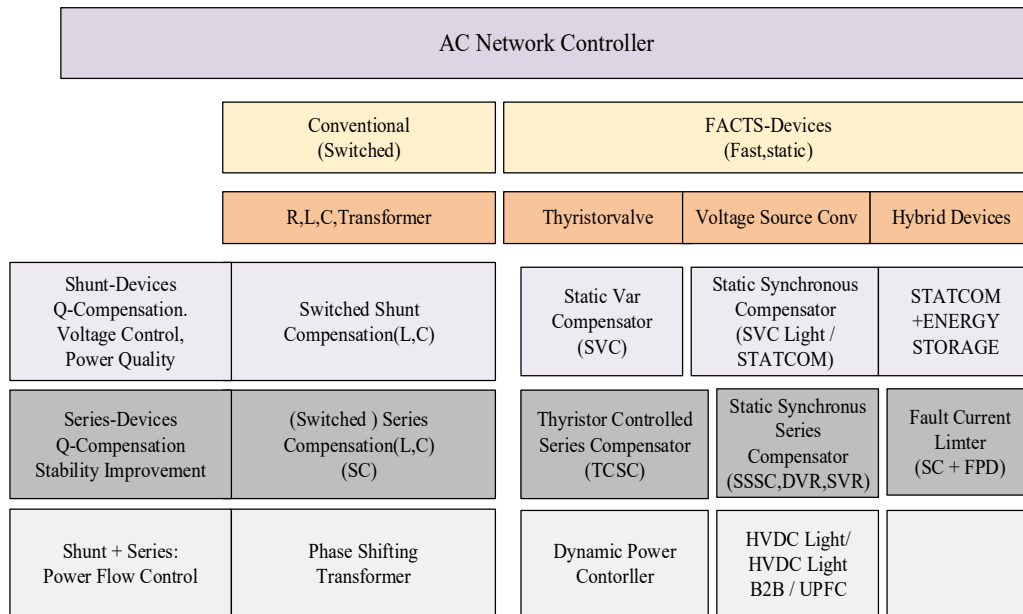


Figure 3-6 Overview of FACTS devices

The traditional devices are made up of fixed or mechanically switchable components like resistance, inductance, or capacitance, as well as transformers. These elements are also present in the FACTS devices, but they are switched in smaller increments or with switching patterns inside an alternating current cycle using additional power electronic valves or converters. Thyristor valves or converters are used in the left column of FACTS devices. These valves, sometimes known as converters, have been around for a long time. Because of their low switching frequency of once per cycle in the converters or the use of Thyristors to simply bridge impedances in the valves, they have negligible losses[29].

The FACTS devices in the right column comprise more advanced voltage source converter technology, which is currently based mostly on Insulated Gate Bipolar Transistors (IGBT) or Insulated Gate Commutated Thyristors (IGCT). Due to a pulse width modulation of the IGBTs or IGCTs, Voltage Source Converters provide a free programmable voltage in magnitude and phase. High modulation frequencies allow for reduced harmonics in the output stream and can even compensate for network interruptions. The downside is that when the switching frequency increases, the losses

increase as well. As a result, unique converter designs are required to compensate for this[29].

3.4 Types of FACTS Controller

FACTS controllers are classified into two types based on whether they are powered by thyristor devices with no gate turn-off capability or by power devices with gate turn-off capability. FACTS controllers are classified into two distinct groups based on their technology[1][30].

- Thyristor-controlled FACTS Controllers which has thyristors with sophisticated controls, much faster response, and with no intrinsic turn-off ability arranged with reactors/ capacitors/. Thyristor Controlled Series Capacitor (TCSC) and Static Var Compensator (SVC) belonged to this group.
- Converter-based FACTS Controllers will have self-commutated voltage-sourced switching converters which can rapidly control static, current sources, or synchronous ac voltage. Static Synchronous Series Compensator (SSSC) and Static Synchronous Compensator (STATCOM) belonged to this group[3], [4].

FACTS devices are classified into the following types based on their location in the transmission network:

- Series controllers

Inject voltage into the line in series. The injected series voltage in the line is defined by the current flowing through the line multiplied by the variable impedance. As long as current and voltage are in phase quadrature, the series controllers supply only reactive power. There are a few series-connected controllers. Thyristor Controlled Series Capacitor (TCSC), Static Synchronous Series Compensator (SSSC), Thyristor Controlled Series Reactor (TCSR), Thyristor Switched Series Capacitor (TSSC), GTO and Phase Angle Regulator (PAR)[1][31].

- Shunt Controllers

Inject current into the line at the connection point. The variable reactive power is consumed or supplied by the shunt controller when the injected current is in phase with the line voltage. Few shunt-connected controllers are Thyristor-controlled Reactor

(TCR), Static Synchronous Compensator (STATCOM), Static Var Compensator (SVC), Thyristor-Switched Reactor (TSR), and thyristor-Switched Capacitor (TSC).

- Combined Series – Shunt Controllers

As they are a combination of series and shunt controllers with coordinated function, inject the voltage in series through the series part and inject current into the line through the shunt part. When they work together as a unified, they can exchange real power.

3.5 Basic Principle and Mode of TCSC Operation

A TCSC is a capacitive reactance that can provide continuous control of power on an alternating current line over a wide range. The principle of variable-series compensation is simply to increase the fundamental-frequency voltage across a fixed capacitor (FC) in a series compensated line by varying the firing angle appropriately. The effective value of the series-capacitive reactance changes as a result of the increased voltage[31].

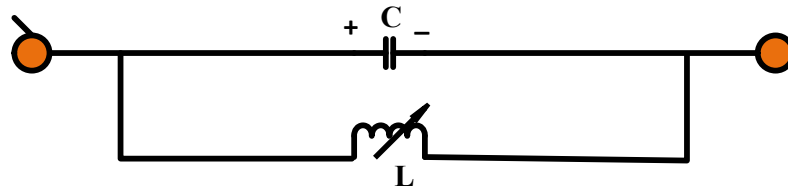


Figure 3-7 Inductor connected in shunt with an FC

Analyzing the behavior of a variable inductor connected in parallel with an FC, as shown in Fig. above, provides a simple understanding of TCSC operation. This LC combination's equivalent impedance, Z_{eq} , is written

$$Z_{eq} = \left(j \frac{1}{\omega C} \right) \parallel (j\omega L) = -j \frac{1}{\omega C - \frac{1}{\omega L}} \quad (3-1)$$

The impedance of the FC alone, however, is given by $-j(1/\omega C)$.

If $\omega C - (1/\omega L) > 0$, or in other words, $\omega L > (1/\omega C)$, the reactance of the FC is less than that of the parallel-connected variable reactor, and this combination provides a variable capacitive reactance is implied. Furthermore, this inductor raises the equivalent capacitive reactance of the LC combination above that of the FC.

If $\omega C - (1/\omega L) = 0$, a resonance develops, resulting in an infinite capacitive impedance, which is unacceptable. On the other hand, $\omega C - (1/\omega L) < 0$, the LC combination provides an inductance greater than the value of the fixed inductor. This situation corresponds to the TCSC's inductive-vernier mode of operation[31].

As the inductive reactance of the variable inductor increases in the variable-capacitance mode of the TCSC, the equivalent-capacitive reactance gradually decreases. For, the minimum equivalent-capacitive reactance is obtained. When the variable inductor is open-circuited or has an extremely large inductive reactance, the value is equal to the reactance of the FC itself[31].

The TCSC behaves similarly to the parallel LC combination. The difference is that the LC-combination analysis is based on the presence of pure sinusoidal voltage and current in the circuit, whereas, in the TCSC, the voltage and current in the FC and thyristor-controlled reactor (TCR) are not sinusoidal due to thyristor switching[31].

There are essentially three modes of TCSC operation[1][31].

3.5.1 Blocked Thyristor Mode

When the thyristor valve is not triggered and the thyristors are kept nonconducting in this mode, the TCSC is operating in blocking mode. The line current is only diverted through the capacitor bank. As a result, the TCSC module is reduced to a fixed-series capacitor, with a capacitive net TCSC reactance. In this mode, the capacitors' dc-offset voltages are monitored and rapidly discharged using a dc-offset control without causing any damage to the transmission-system transformers[1][31].

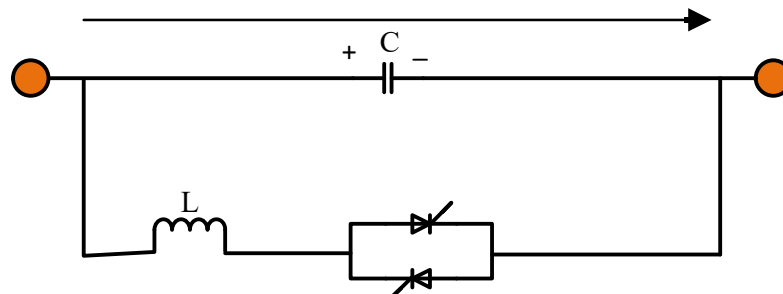


Figure 3-8 Blocked Thyristor Mode

3.5.2 Bypassed Thyristor Mode

The thyristors are made to fully conduct with a conduction angle of 180 degrees in this bypassed mode. When the voltage across the thyristors reaches zero and becomes positive, gate pulses are applied, resulting in a continuous sinusoidal flow current through the thyristor valves. When the thyristor valve is continuously triggered, the valve remains to conduct at all times, and the TCSC acts as a parallel connection of the series capacitor bank with the inductor in the thyristor valve[30][31].

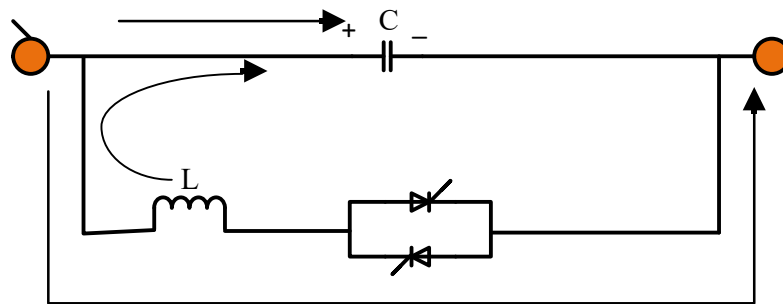


Figure 3-9 Bypassed Thyristor Mode

3.5.3 Partially Conducting Thyristor or Vernier Mode

This mode allows the TCSC to operate as either a continuously controllable capacitive reactance or a continuously controllable inductive reactance. It is accomplished by varying the firing angle of the thyristor pair in a suitable range. However, due to the resonant region between the two modes, a smooth transition from capacitive to inductive mode is not possible[30], [31].

The capacitive-vernier-control mode is a variant of this model in which the thyristors are activated when the capacitor voltage and current have opposite polarity. This condition causes a TCR current to flow in the opposite direction of the capacitor current, resulting in a loop-current flow in the TCSC controller[30], [31].

The loop current raises the voltage across the FC, effectively increasing the equivalent capacitive reactance and series compensation level for the same line current value.

To avoid resonance, the firing angle α_{\min} of the forward-facing thyristor is constrained in the range $\alpha_{\min} \leq \alpha \leq 180^\circ$ as measured from the positive reaching a zero crossing of the capacitor voltage. This constraint allows for continuous vernier control of the TCSC

module's reactance. As α is reduced from 180° to α_{\min} , the loop current increases. The maximum TCSC reactance allowed with $\alpha = \alpha_{\min}$ is typically two and a half to three times the capacitor reactance at the fundamental frequency[30], [31].

Another variant is the inductive-vernier mode, which allows the TCSC to be operated with a high level of thyristor conduction. The circulating current is reversed in this mode, and the controller has a net inductive impedance.

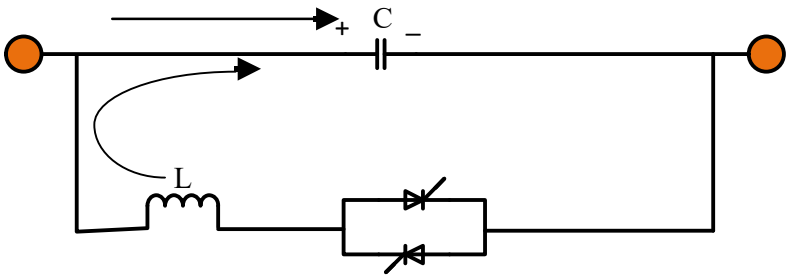


Figure 3-10 Partially Conducting Thyristor Capacitive Vernier

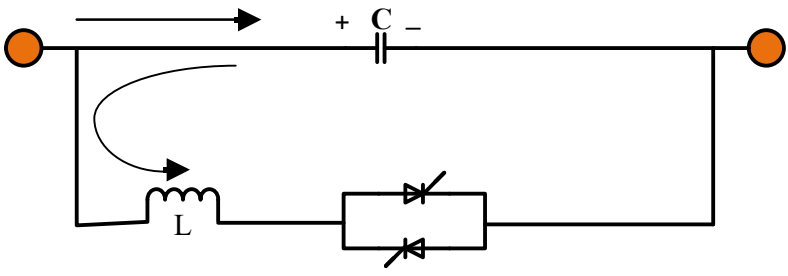


Figure 3-11 Partially Conducting Thyristor Inductive Vernier

Based on the simplified TCSC circuit shown in the figure below, the analysis of TCSC operation in the vernier-control mode is performed.

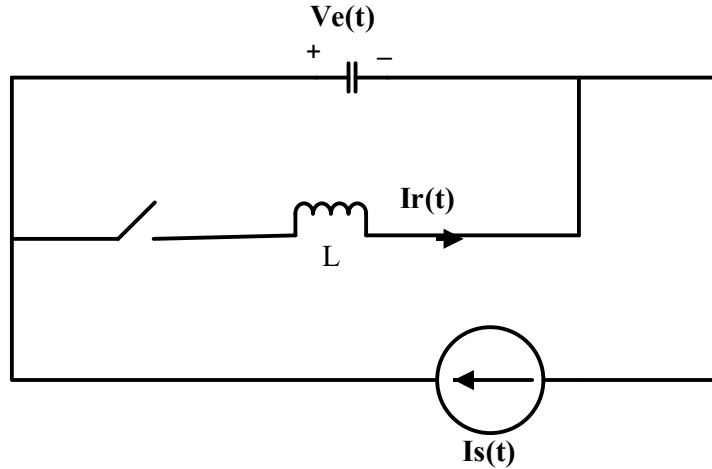


Figure 3-12 Simplified TCSC circuit

Based on the simplified TCSC circuit shown in the figure below, the analysis of TCSC operation in the vernier-control mode is performed. Transmission-line current is assumed to be the independent input variable and is represented as an external current source, $i_s(t)$.

The current through the fixed-series capacitor, C , is expressed as

$$C \frac{dv_c}{dt} = i_s(t) - i_T \cdot u \quad (3-2)$$

When the thyristor valves are conducting, that is, when the switch S is closed, the switching variable $u = 1$. When the thyristors are not blocked, that is, when switch S is open, $u = 0$.

$i_t(t)$, the thyristor-valve current, is then described

$$L \frac{di_t}{dt} = v_c \cdot u \quad (3-3)$$

The line current, $i_s(t)$, be represented by

$$i_s(t) = I_m \cos \omega t \quad (3-4)$$

By solving equations 3.2 and 3.3 with the knowledge of instant switching. For balanced TCSC operation using equidistant firing-pulse control, the thyristors are turned on twice in each cycle of line current at instants t_1 and t_3 , given by

$$t1 = -\frac{\beta}{\omega} \quad (3-5)$$

$$t3 = \frac{\pi - \beta}{\omega} \quad (3-6)$$

Where β is the angle of advance

$$\beta = \pi - \alpha; 0 < \beta < \beta_{max} \quad (3-7)$$

A reference signal that is in phase with the capacitor voltage is used to generate the firing angle α . The thyristor switch S turns off at the instants $t2$ and $t4$, defined as

$$t2 = t1 + \frac{\sigma}{\omega} \quad (3-8)$$

$$t4 = t3 + \frac{\sigma}{\omega} \quad (3-9)$$

Where σ denotes the conduction angle, which is assumed to be the same in both the positive and negative conduction cycles. Also,

$$\sigma = 2\beta \quad (3-10)$$

Solving the TCSC equation 3.2 – 3.4 results in the steady-state thyristor current, i_T , as

$$i_T(t) = \frac{k^2}{k^2 - 1} \text{Im} \left[\cos \omega t - \frac{\cos \beta}{\cos k\beta} \cos \omega_r t \right]; -\beta \leq \omega t \leq \beta \quad (3-11)$$

Where

$$\omega_r = \frac{1}{\sqrt{LC}} \quad (3-12)$$

$$k = \frac{\omega_r}{\omega} = \sqrt{\frac{1}{\omega L} \cdot \frac{1}{\omega C}} = \sqrt{\frac{X_C}{X_L}} \quad (3-13)$$

X_C denotes the nominal reactance of the FC alone. The steady-state capacitor voltage at the instant $\omega t = -\beta$ is expressed by

$$v_{c1} = \frac{\text{Im}X_C}{k^2 - 1} (\sin \beta - k \cos \beta \tan k\beta) \quad (3-14)$$

At $\omega t = \beta$, $i_T = 0$, and the capacitor voltage is given by

$$v_c(\omega t = \beta) = v_{c2} = -v_{c1} \quad (3-15)$$

Finally, the capacitor voltage is given by

$$v_{c(t)} = \frac{\text{Im}X_c}{K^2 - 1} \left(-\sin \omega t + K \frac{\cos \beta}{\cos k\beta} \sin \omega_r t \right); \quad (3-16)$$

$$-\beta \leq \omega t \leq \beta$$

$$v_{ct} = v_{c2} + \text{Im} X_c (\sin \omega t - \sin \beta); \quad (3-17)$$

$$\beta < \omega t < \pi - \beta$$

The fundamental component, V_{cf} , is obtained as

$$V_{cf} = \frac{4}{\pi} \int_0^{\pi/2} v_c(t) \sin \omega t \, d(\omega t) \quad (3-18)$$

The equivalent TCSC reactance is calculated as the V_{cf}/Im :

$$\begin{aligned} X_{\text{TCSC}} = \frac{V_{cf}}{\text{Im}} = X_c - \frac{X_c^2}{(X_c - X_L)} \frac{2\beta + \sin 2\beta}{\pi} \\ + \frac{4X_c^2}{(X_c - X_L)} \frac{\cos^2 \beta}{(K^2 - 1)} \frac{(K \tan K\beta - \tan \beta)}{\pi} \end{aligned} \quad (3-19)$$

The TCSC's net reactance in units of X_c , given by $X_{\text{net}} = (X_{\text{TCSC}}/X_c)$, derived as

$$\begin{aligned} X_{\text{net}} \quad (3-20) \\ = 1 - \frac{X_c}{(X_c - X_L)} \frac{\sigma + \sin \sigma}{\pi} \\ + \frac{4X_c}{(X_c - X_L)} \frac{\cos^2(\sigma/2)}{(K^2 - 1)} \cdot \frac{[\text{ktan}(\frac{k\sigma}{2}) - \tan(\sigma/2)]}{\pi} \end{aligned}$$

Where

$$K = \sqrt{\frac{X_c}{X_L}} = \text{compensation ratio} \quad (3-21)$$

$$\sigma = 2(\pi - \alpha) = \text{Conduction angle of TCSC Controller} \quad (3-22)$$

$$X_c = \text{Capacitor reactance} \quad (3-23)$$

$$X_L = \text{Inductor reactance} \quad (3-24)$$

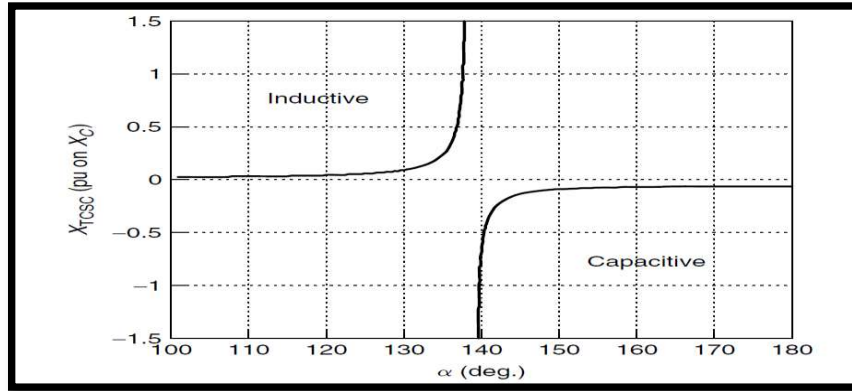


Figure 3-13 Impedance Vs Firing Angle Characteristics Curve

According to equation (3.20), changing the firing angle of a bidirectional thyristor can control the TCSC reactance value (X_{TCSC}).

If the firing angle is 90° or greater, X_{TCSC} can be minimal. In contrast, if a minimum firing angle is given, X_{TCSC} will be at its maximum. Figures 3-8 depict the impedance characteristics of a TCSC with a thyristor firing angle.

A parallel resonance at the fundamental frequency is formed between X_C and X_L , corresponding to the values of firing angle α_{res} given by

$$\alpha_{res} = \pi - (2m - 1) \frac{\pi\omega}{2\omega r} ; m = 1,2 \quad (3-25)$$

Or

$$\beta_{res} = (2m - 1) \frac{\pi\omega}{2\omega r} ; m = 1,2 \quad (3-26)$$

The various resonances can be reduced to one by selecting an appropriate value of $K = \left(\frac{\omega_r}{\omega}\right)$ in the range $90^\circ < \alpha < 180^\circ$ or $0 < \beta < 90^\circ$

The TCSC has a very large impedance at the resonant point, resulting in a significant voltage drop. This resonant region is avoided by limiting the firing angle. The firing angle that results in resonance is typically 145 degrees. Filters are provided in the synchronizing and timing circuits to ensure that any transients or distortions in the alternating current system voltage do not affect the performance of the TCSC control system. Nonetheless, the TCSC's vernier operation can only increase apparent reactance in both capacitive and inductive domains. The TCSC will not be able to reduce the reactance[31].

3.6 TCSC Layout and Protection

In the basic conceptual TCSC module, a series capacitor, C, is connected in parallel with a thyristor-controlled reactor, LS, as shown in figure 3.5 a). In contrast, a practical TCSC module includes protective equipment, which is typically installed with series capacitors. as shown in figure 3.5 b)[31].

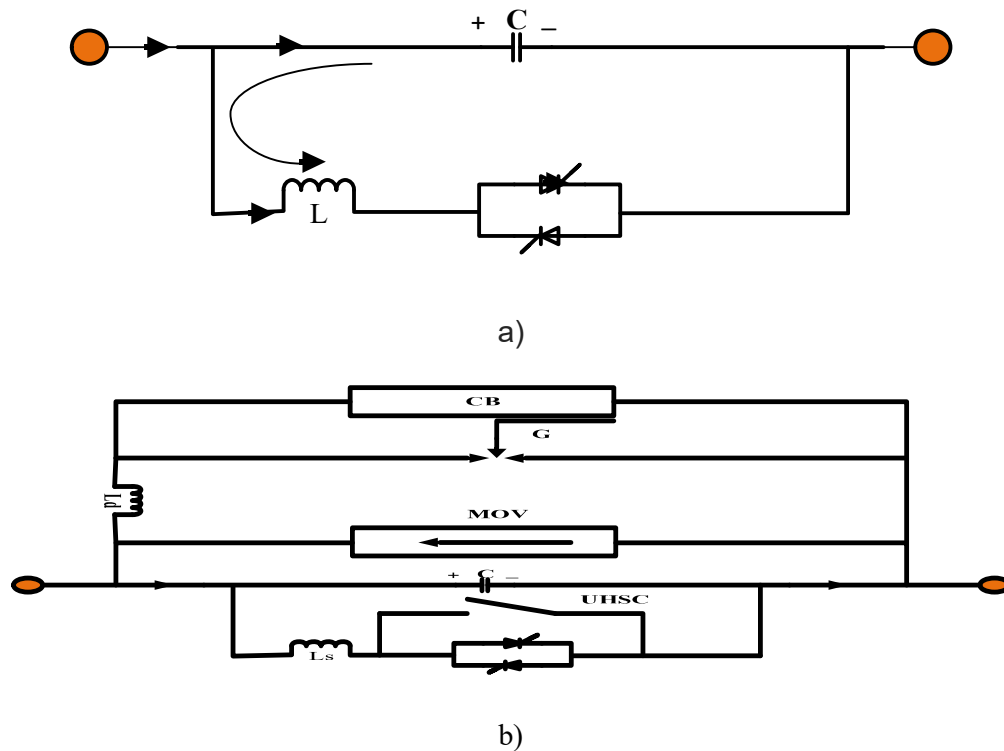


Figure 3-14 FACTCS Module a) a basic module b) a practical module [31]

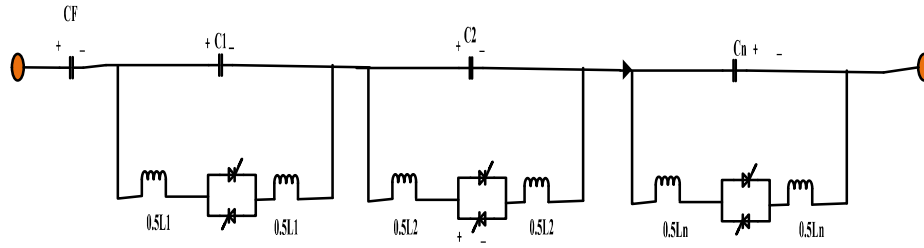


Figure 3-15 Typical TCSC System [6]

To prevent high-capacitor overvoltage, a metal-oxide varistor (MOV), which is essentially a nonlinear resistor, is connected across the series capacitor. The MOV not only limits the voltage across the capacitor but also allows the capacitor to remain in the circuit even during fault conditions, which improves transient stability.

A circuit breaker, CB, is also installed across the capacitor to control its insertion into the line. Furthermore, if a severe fault or equipment malfunction occurs, the CB bypasses the capacitor. In the circuit, a current-limiting inductor, L_d , is used to limit both the magnitude and frequency of the capacitor current during the capacitor-bypass operation.

If the TCSC valves should first operate in the fully "on" mode for an extended period, conduction losses are reduced by installing an ultra-high-speed contact (UHSC) across the valve. This metallic contact, like circuit breakers, has a virtually lossless feature and can handle a wide range of switching operations. The metallic contact closes shortly after the thyristor valve is activated and opens shortly before the valve is deactivated. The metallic contact is closed to relieve stress on the valve during a sudden overload of the valve, as well as during fault conditions.

An actual TCSC system is typically made up of a cascaded combination of many such TCSC modules, as well as a fixed-series capacitor, CF. This fixed series capacitor is primarily designed to decrease costs. Figure 3.6 illustrates a conceptual TCSC system with basic TCSC modules. To provide a wider range of reactance control, the capacitors C1, C2, and Cn in the various TCSC modules may have different values. To protect the thyristor valves from inductor short circuits, the inductor in series with the antiparallel thyristors is split into two halves.[31]

3.7 TCSC Capability Characteristics

Even though TCSC design is based on application requirements, the operational limits are determined by the characteristics of various TCSC components. The following are some of the most important constraints:[1], [31].

- Voltage Limits

Voltage may vary with the duration of voltage application. The overvoltage limit of the MOV is more critical than that of the capacitor.

- Current Limits

High currents can affect the operation of a TCSC, and they may need to be imposed on the currents in the valve, FC, and surge inductor to prevent overheating. Harmonics also causes heating, which restricts the TCSC's operation.

- Firing Angle Limits

The thyristors must be tightly controlled to prevent the TCSC from entering the resonant region

3.8 TCSC Losses

The following are the TCSC losses:

- The thyristor-conduction losses
- The switching losses
- The series capacitor losses
- The reactor conduction losses

The study's aim is to enhance the power transfer capability of a 230 Kv transmission line from Legetafo to Debre Birhan by determining the best location and size of TCSC. Furthermore, check the merit of TCSC by conducting a cost-benefit analysis.

CHAPTER FOUR

4 Methodology (materials and methods)

4.1 Data Collection and analysis

The data for this study was collected from the Ethiopian electric power EEP project team's head office, the EEP Debre Birhan substation, and the Ethiopian central statistics agency. This chapter contains a variety of data for the design of TCSC to improve power handling capacity. In this work, the proposed of three input layers: historical load data, GDP, and energy metering devices, and one output layer Peak Load (PL). The ANN function in Matlab is used to forecast load.

- Historical Load data, GDP, and number of energy metering devices

Data on historical load and the number of energy metering devices is gathered from the Debre Birhan Substation and the Ethiopia Electric Utility, Debre Birhan District. GDP data is obtained from the World Bank's web portal.

(https://data.worldbank.org/indicator/NY.GDP.MKTP.KD.ZG?locations=ET&most_recent_year_desc=true).

All the stated data above is shown in the table 4-1.

Year(E.C)	Peak Load (MW)	GDP %	Number of Energy Metering Devices
2017	125	9.5	12145
2018	140	6.8	14673
2019	152	8.3	15452
2020	186	6.1	17136
2021	194	2	18456

Table 4-1 Input layers data

- Transmission line data

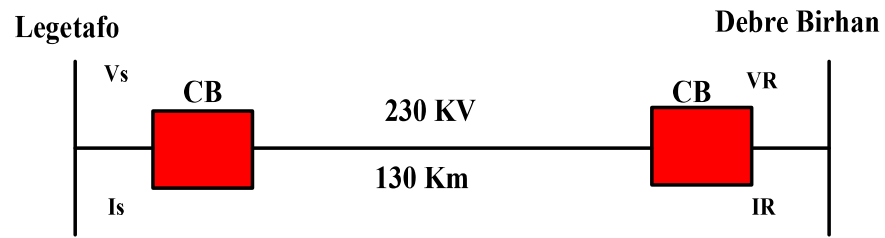


Figure 4-1 Single Line Diagram of Transmission Line

medium-length transmission-line approximations are presented as a method of introducing ABCD parameters. A transmission line is easily represented by the two-port network shown in Figure 4-1, where V_S and I_S represent the sending-end voltage and current, and V_R and I_R represent the receiving-end voltage and current. The relationship between the quantities at the sending and receiving ends can be written as[32].

$$V_s = AV_R + BI_R \text{ Volts} \quad (4-1)$$

$$I_s = CV_R + DI_R \text{ A} \quad (4-2)$$

Or in matrix form

$$\begin{bmatrix} V_S \\ I_S \end{bmatrix} = \begin{bmatrix} A & B \\ C & D \end{bmatrix} \begin{bmatrix} V_R \\ I_R \end{bmatrix} \quad (4-3)$$

where A, B, C, and D are parameters influenced by the transmission-line constants R, L, C, and G

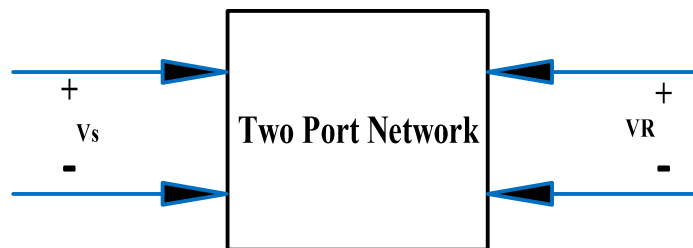


Figure 4-2 Representation of two-port network

The transmission line connecting Legetafo and Debre Birhan is categorized as a medium transmission line. Thus, transmission length, impedance characteristics, voltage level, maximum capacity, conductor arrangement or configuration, tower height, the distance between conductors, type, and manufacturer of transmission lines are all data are stated below on table 4-2.

Voltage (kV)	Conductor	Tower Config.	No. Con	Positive Sequence			Zero Sequence		
				R	X	B	R0	X0	B0
				Ω/km	Ω/km	$\mu S/km$	Ω/km	Ω/km	$\mu S/km$
230	Twin Ash	Single	2	0.1067	0.3261	3.5224	0.3469	1.0382	2.1530

Table 4-2 Transmission Line Data

Total series impedance can be evaluated as shown below

$$z = R + j\omega L \frac{\Omega}{Km}, \text{ series impedance per unit length} \quad (4-4)$$

$$y = G + j\omega C \frac{S}{Km}, \text{ shunt admittance per unit length} \quad (4-5)$$

$$Z = zl \Omega, \text{ total series impedance} \quad (4-6)$$

$$Y = yl S, \text{ total shunt admittance} \quad (4-7)$$

$$l = \text{line length Km} \quad (4-8)$$

- Substation data

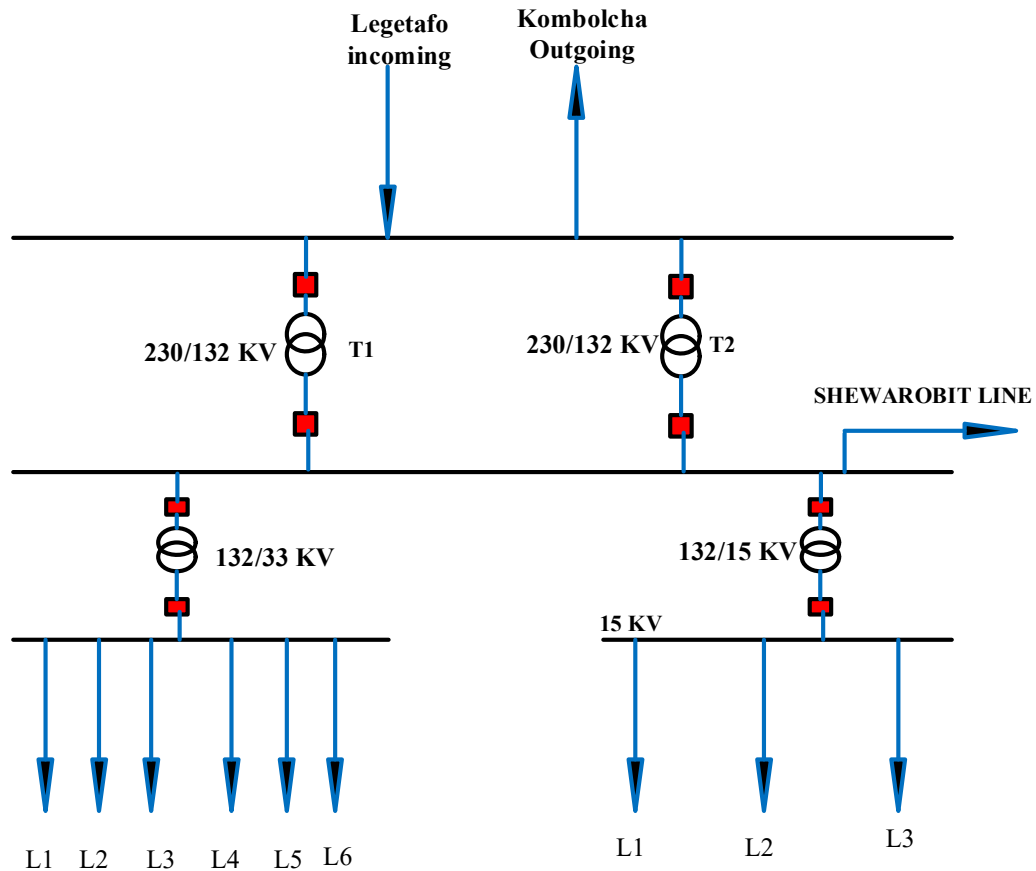


Figure 4-3 Single-Line Diagram of Debre Birhan Substation

Debre Birhan substation is located in Debre Birhan town, North Shewa, Ethiopia, which incorporates many industrial and commercial loads. All loads were supplied by the Debre Birhan substations, which are located in Debre Birhan. The layout diagram of the Debre Birhan substation is illustrated in Figures 4-3. The Debre Birhan substation has one incoming 230 KV line from Legetafo and one outgoing 230 KV line to Kombolcha respectively. The feeder is configured radially with a voltage level of 33 kV and 15 kV. There are 6 outgoing 33 KV feeders in Debre Birhan Town, Enewarie, Sheno, Ginper Glass Industry, Boortmal Factory, and Debre Birhan Industry park. And also 3 outgoing 15 KV feeders Debre Birhan Town Kebele 02, Mendida, and Wan Way Textile. The data is collected from Debre Birhan Substation by going from the site and collected from SCADA systems and log sheets.

The sample data of the Debre Birhan substation voltage profile, the Debre Birhan substation receiving end active power (MW), the Debre Birhan substation receiving end reactive power (MVAR), and the Debre Birhan substation receiving end power factor are stated in Appendix D to Appendix G.

4.2 Software used for modeling.

The software MATLAB/R2019a/SIMULINK/simscape was used in this study. It is a comprehensive scientific computing environment that is almost straightforward to use. It provides an interactive system for engineers, researchers, and scientific studies that integrates a variety of scientific numerical computation and visualization algorithms. It is a powerful and programmable system that allows for particularly impressive gains in productivity and efficiency.

4.3 Model of the System without TCSC

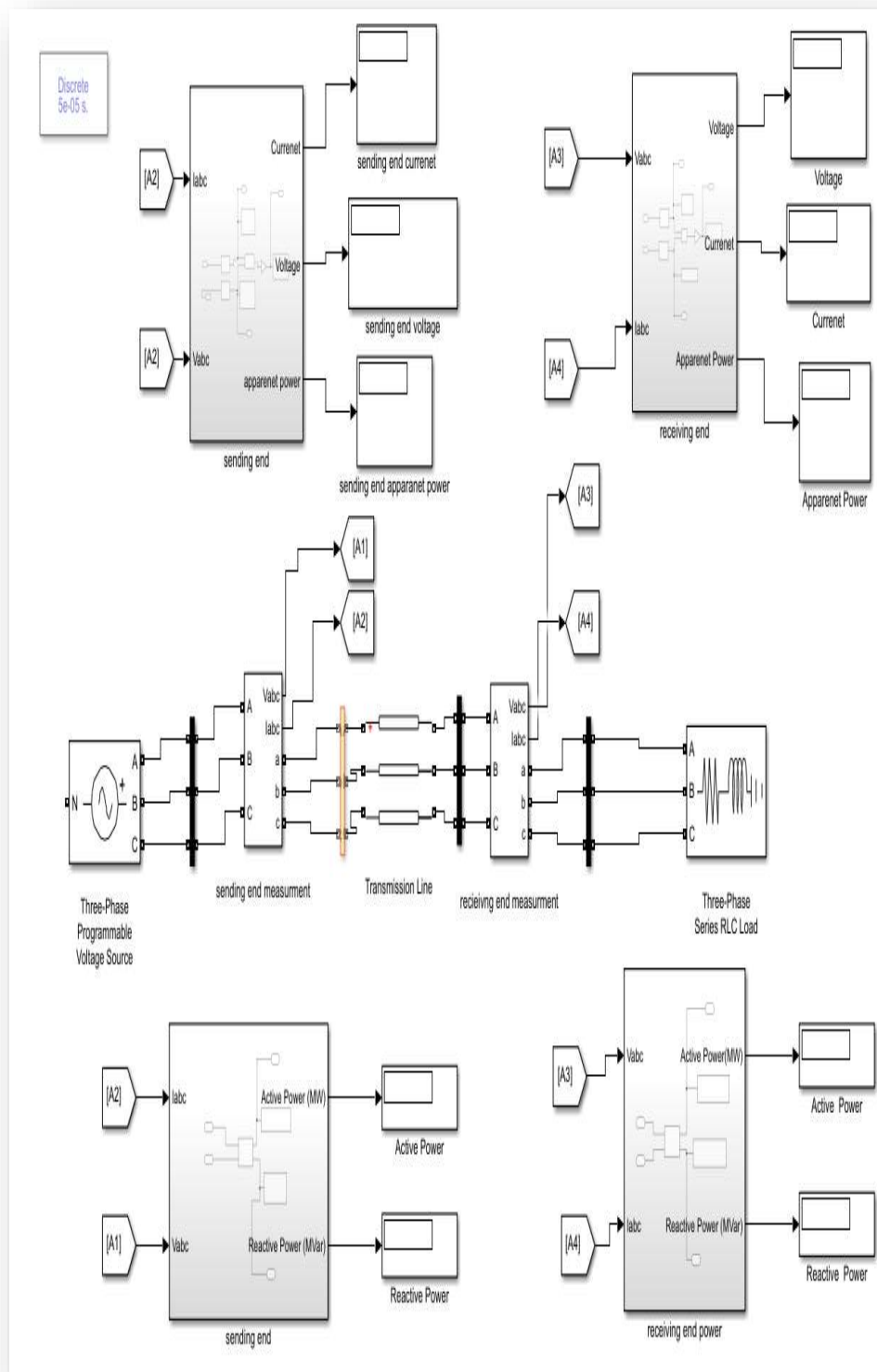


Fig 4-4 Model of the system without TCSC

CHAPTER FIVE

5 Result and Discussion

In this chapter, different results were obtained and presented. All the relevant parameters are given in the appendix. The source voltage of 230 Kv is connected by a 130 Km transmission line. The TCSC used for this model is a detailed model.

5.1 Forecasting Future Load Demand through ANN

The topic of ANN is well covered in Chapter 3, so it will not be discussed further here. A utility's previous electrical demand must be represented by several data points. The previous load data and energy metering devices are the most important. ANN was trained using historical data from annual peak loads, energy measurement devices, and GDP. There will be a five-year period from 2017 to 2021. These numbers will also be used to forecast the peak load between 2022 and 2027. Matlab 2019a is used for all simulations.

ANN implementation method is as follows

- Three training data points are provided to the ANN
- A feed-forward structure is used to obtain the corresponding network outputs.
- Using the least square error method, the network weights are updated based on the difference between the desired and actual output

Input				Target
NO	Year	GDP (%)	Energy Metering Devices	Peak Load (MW)
1	2017	9.5	12145	125
2	2020	6.1	17136	186
3	2021	2	18456	194

Table 5-1 Input-Output training pattern

Input				Target
NO	Year	GDP (%)	Energy Metering Devices	Peak Load (MW)
1	2018	6.8	14673	140
2	2019	8.3	15452	152

Table 5-2 Input-Output Testing Pattern

Training and Testing Performance

In Matlab, ANN can be constructed either nntool or nntstart. In this work, nntool has been used.

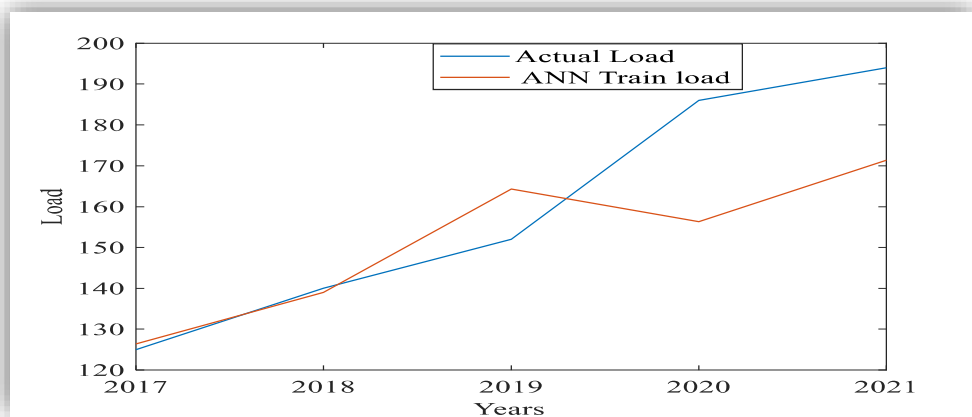


Figure 5-1 Training Pattern Vs Actual Output

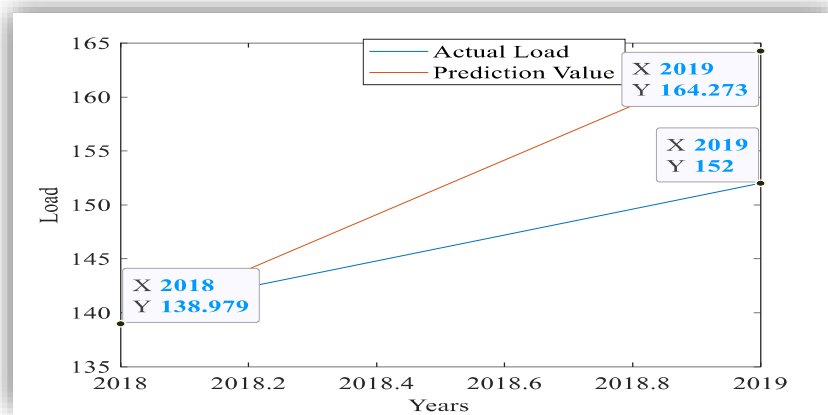


Figure 5-2 Testing Pattern Vs Actual Output

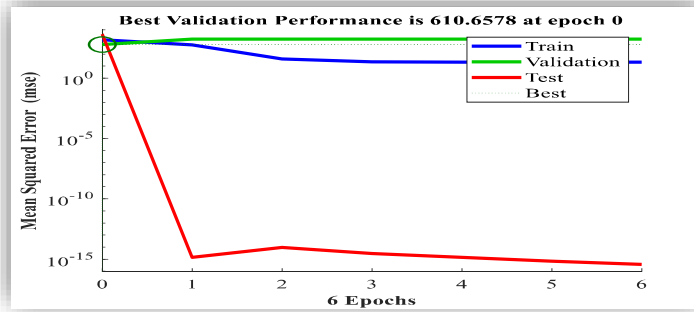


Figure 5-3 Validation Performance

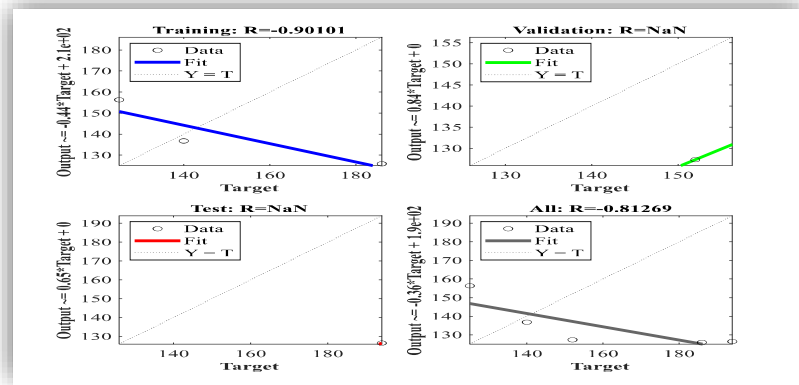


Figure 5-4 Regression Plot

The result of peak load forecasting by ANN for the years 2022 to 2026 are presented below

Year	Forecasting Load (MW)
2022	212
2023	231
2024	251
2025	275
2026	304

Table 5-3 peak load Forecasted

5.2 Simulink Model of TCSC for 230 KV Transmission Line

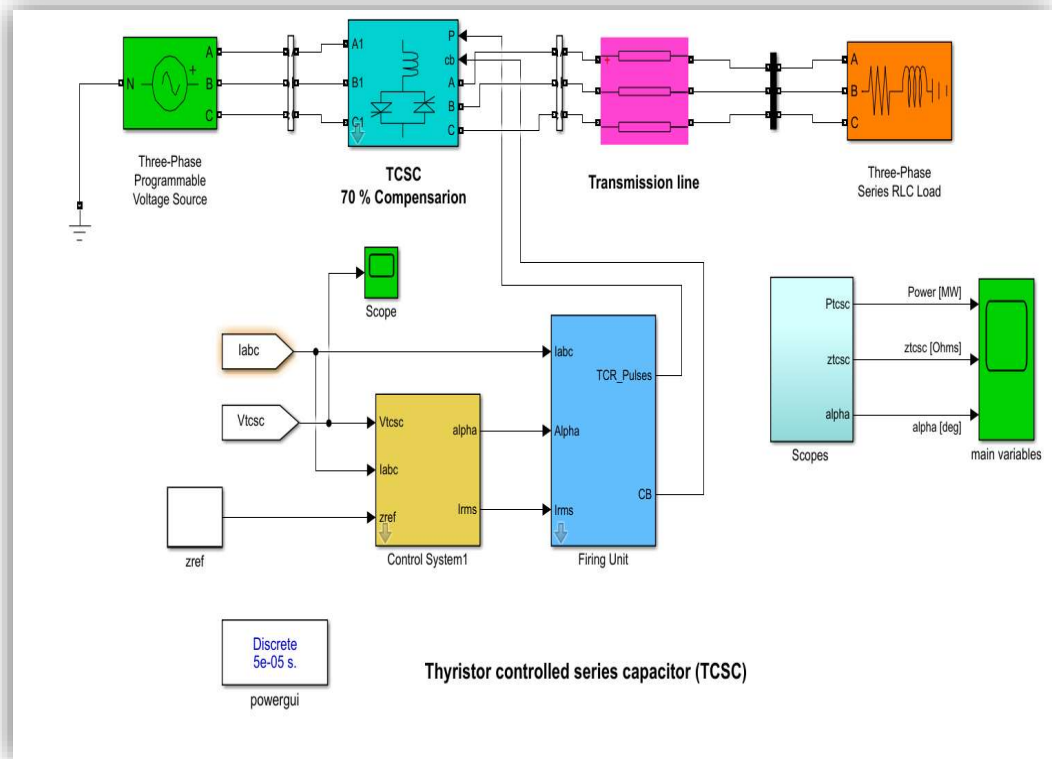


Figure 5-5 Simulink model of transmission line with TCSC installed at the sending end

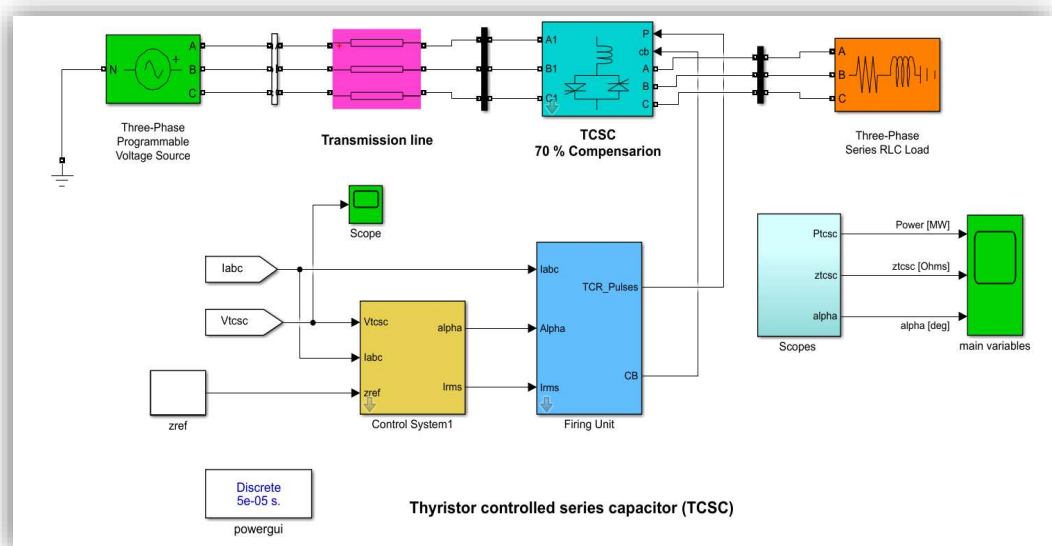


Figure 5-6 Simulink model of transmission line with TCSC installed at the receiving end

5.3 TCSC Placement and Sizing

5.3.1 Sizing of TCSC

The design criteria for determining the value of the inductor and capacitor for TCSC are determined by the transmission line's net reactance and the power flow through the line [33]–[35].

The value of the capacitor is determined by the degree of series compensation (K). Typically, up to 70% of the line reactance is chosen for compensation. As a result, the maximum capacitive compensating reactance that the TCSC can provide is 70 % of the line reactance[1], [31], [36], [37]. The choice of the inductor is determined by the length of the operating area required for the inductive and capacitive regions.

Three major significant measures must be considered when selecting a capacitor and inductor for a TCSC device [1], [36], [37].

- i. Degree of series compensation
- ii. Inductive reactance, X_L should be sufficiently smaller than capacitive reactance, X_C
- iii. Occurrence of the multi resonance condition

A resonance region exists between the inductive and capacitive regions. It is unavoidable for resonance to occur in a TCSC device. However, only one resonant region is permitted, namely one capacitive range and one inductive range. The TCSC's operating range will be reduced if there are multiple resonant points. According to the formula (4-4)

$$z = 0.106 + 0.3261 \frac{\Omega}{Km} \quad (5-1)$$

Equation (4-7) can be used to calculate the total series impedance.

$$Z = \left(0.106 + 0.3261 \frac{\Omega}{Km} \right) * 130Km \quad (5-2)$$

$$Z = (13.87 + j 42.393) \Omega \quad (5-3)$$

In this paper, the TCSC is modeled for a transmission line reactance of 42.393 Ω .

$$X_{line} = 42.393 \Omega \quad (5-4)$$

$$X_{TCSCmax} = 70 \% \text{ of } X_{line} = 42.393 * 0.7 = 29.6751 \Omega \quad (5-5)$$

X_{order} is a measure of how well TCSC can provide capacitive compensating reactance over the reactance value of its internal capacitor. In most cases, $X_{order} \leq 3$ [33].

$$X_{order} = \frac{X_{TCSCmax}}{X_c} \quad (5-6)$$

Consider the case where $X_{order} = 3$. As a result, X_c can be calculated as

$$X_c = \frac{X_{TCSCmax}}{X_{order}} = \frac{29.6751}{3} = 9.8917 \Omega \quad (5-7)$$

$$C = \frac{1}{2\pi f X_c} = \frac{1}{2 \times 3.14 \times 50 \times 9.8917} = 321.9581 \mu F \quad (5-8)$$

The inductive reactance of the TCSC's inductor is calculated as [33].

$$X_L = 0.15 \times X_c = 1.483 \Omega \quad (5-9)$$

$$L = \frac{X_L}{2\pi f} = 1.89 \text{ mH} \quad (5-10)$$

Simulation Parameters	Values
Transmission Line	$(13.87 + j 42.393) \Omega$
Total number of TCSC	1
TCSC capacitance and reactance	$C = 321.9581 \mu F$; $L = 1.89 \text{ mH}$

Table 5-4 Simulation Parameters

5.3.2 TCSC Placement

There are three options for optimal TCSC placement on a transmission line:

- i. Sending end of the transmission line
- ii. In the middle of the transmission line
- iii. At the receiving end of the transmission line

The IEEE standards for TCSC details have been subjected to various analyses, and TCSC performs better when installed on the sending or receiving end [16].

The simulation is carried out in this paper by first placing the TCSC on the sending end of the transmission line and then on the receiving end of the transmission line.

5.4 Controller System

To control TCSC, one of two types of control (closed-loop or open-loop) can be used [31]. Open-loop control is used to generate an output based on a predefined transfer function without the need for response measurement, while closed-loop control denotes a conventional feedback system. Reactive power compensator controllers are typically based on one of three modes: constant current (CC), constant angle (CA), or constant power (CP)

The proposed study employs closed-loop control, with both load current and voltage traced as feedback, and the slope of the voltage/current characteristic is determined by the ratio of compensator current to voltage error. The controller in this paper is designed in capacitive and inductive control modes using a separate fuzzy logic controller.

The TCSC control block parameter represents the impedance measured and referenced, when TCSC is in constant impedance mode, it calculates the TCSC impedance using voltage and current feedback. the reference impedance indirectly determines the power level. In each operating mode, a separate Fuzzy Logic controller is used.

In each phase, the TCSC is simulated as a controllable voltage source. The magnitude of the voltage is the product of the equivalent complex impedance and the line current.

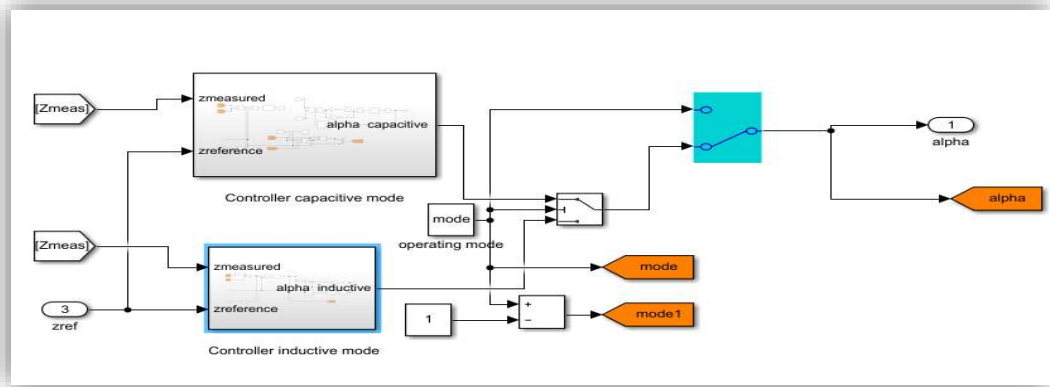


Figure 5-7 TCSC control system diagram

5.4.1 PI Controller

As the simplest closed-loop controller, a conventional PI controller is used to determine the firing angle and control the transmitted power. First, the power error signal, which is the difference between the reference and measured impedances, is used for this purpose.

The TCSC analytical modeling is placed in Matlab [38], and the diagram consists of a PI controller, a PI controller for regulating alpha in capacitive mode, and also a PI controller for regulating alpha in inductive mode.

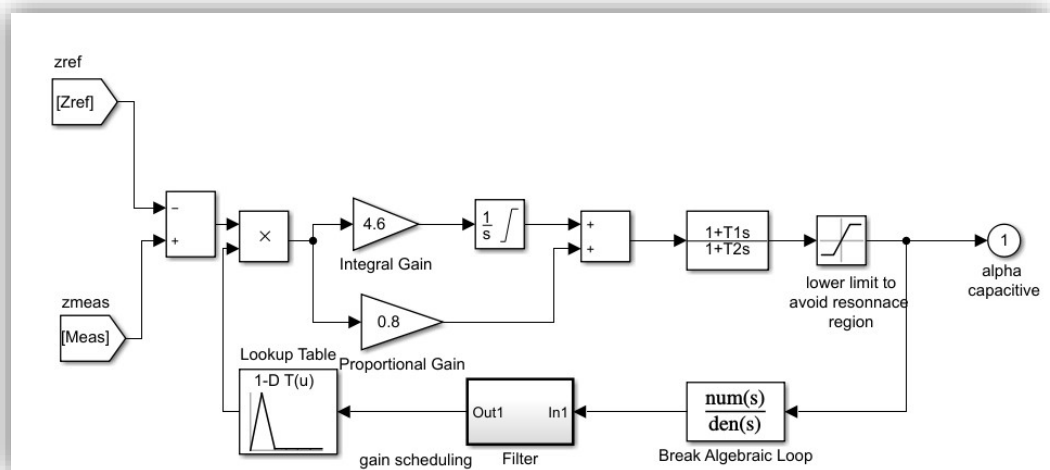


Figure 5-8 PI Controller of TCSC

5.4.2 Fuzzy Logic Controller

Fuzzy logic is a control approach with a lot of real-time potential [39], [40]. A fuzzy logic controller is a rule-based controller in which a set of rules represents a control decision mechanism for correcting the effect of certain power system causes.

Depending on the control type, the error (input) can be selected as current, voltage, or impedance. The input in our scenario is impedance. The angle signal is the output of the fuzzy logic controller, and the pulse generator provides firing pulses to the thyristors. This work presents a fuzzy capacitive and inductive mode controller, for controlling alpha in both capacitive and inductive mode using ANFIS inference.

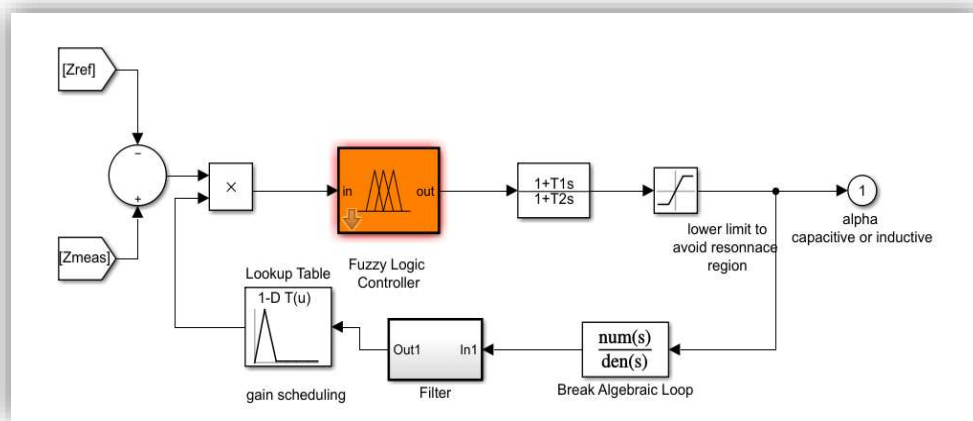


Figure 5-9 Fuzzy Logic Controller of TCSC

5.4.2.1 Fuzzy capacitive mode controller.

Ten fuzzy sets of input data and eight fuzzy sets of output values are tested using the input and output membership functions, which are both given below. A triangular membership function is used, and all fuzzy implications are based on Mamdani's fuzzy inference.

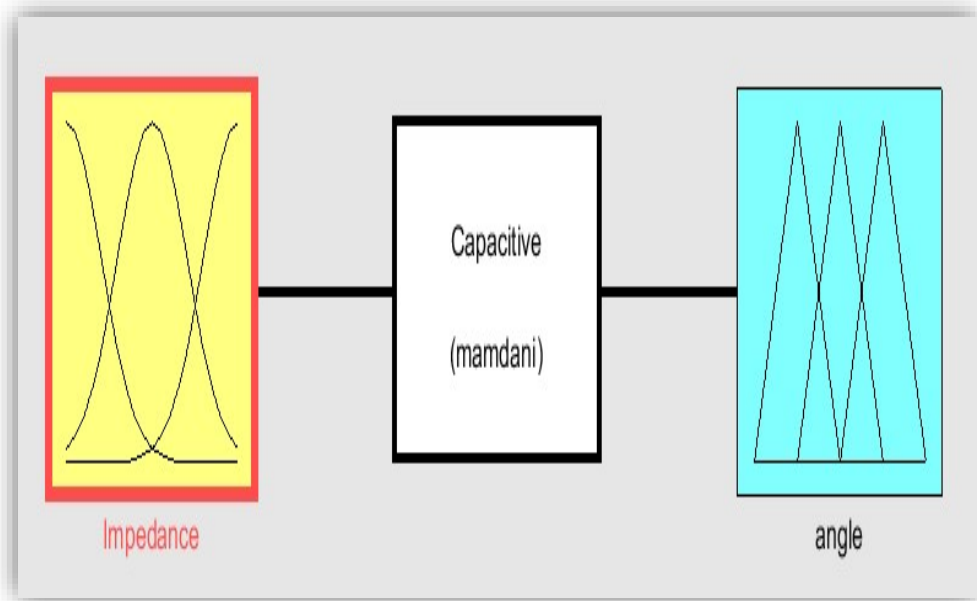


Figure 5-10 Capacitive Mode Mamdani Fuzzy Interface

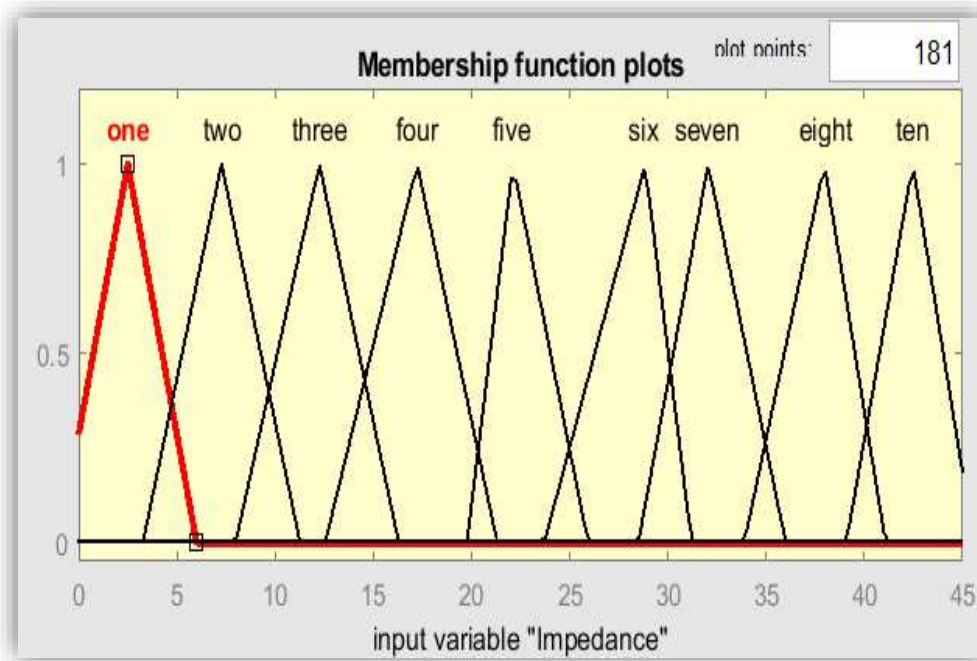


Figure 5-11 Capacitive Mode Input Membership Function

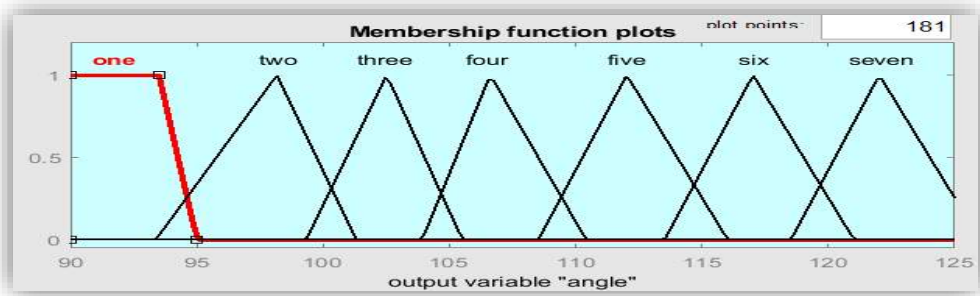


Figure 5-12 Capacitive Mode Output Membership Function

According to figure 5-10, there are nine rules in the fuzzy controller including;
 If the input membership function is one (extra small) then the output membership function is also one (extra small)

5.4.2.2 Fuzzy inductive mode controller.

Six fuzzy sets of input data and seven fuzzy sets of output values are tested using the input and output membership functions, which are both given below. A triangular membership function is used, and all fuzzy implications are based on Mamdani's fuzzy inference. There are six rules in the fuzzy controller.

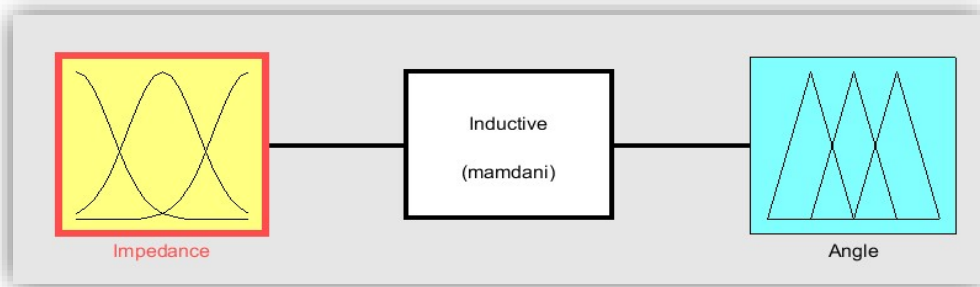


Figure 5-13 Inductive Mode Mamdani Fuzzy Interface

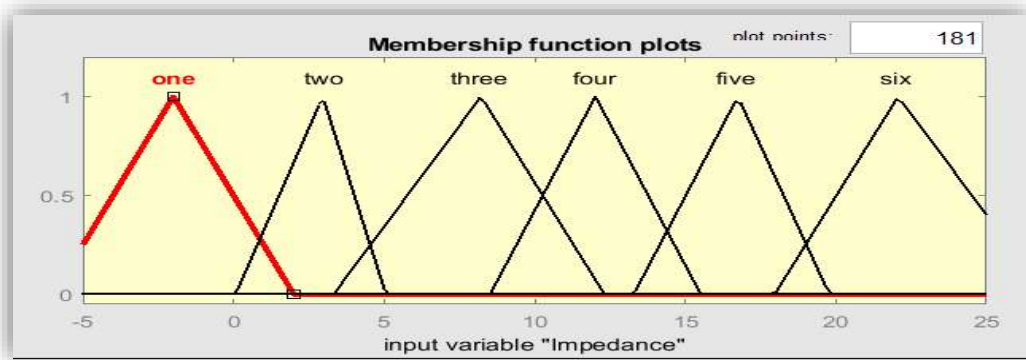


Figure 5-14 Inductive Mode Input Membership Function

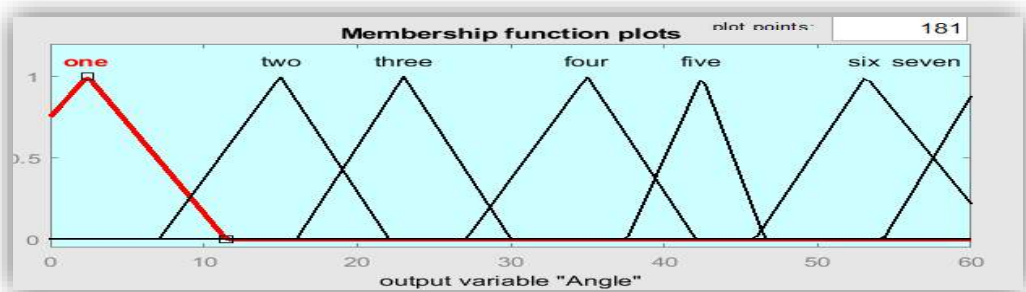


Figure 5-15 Inductive Mode Output Membership Function

According to figure 5-13, there are six rules in the fuzzy controller including;
 If the input membership function is one (extra small) then the output membership function is a (extra High)

5.5 Firing unit

In the firing unit, the line current is synchronized using closed-loop control and then compared, and the zero crossing of the line current is checked to generate a square wave and synchronize the pulses.

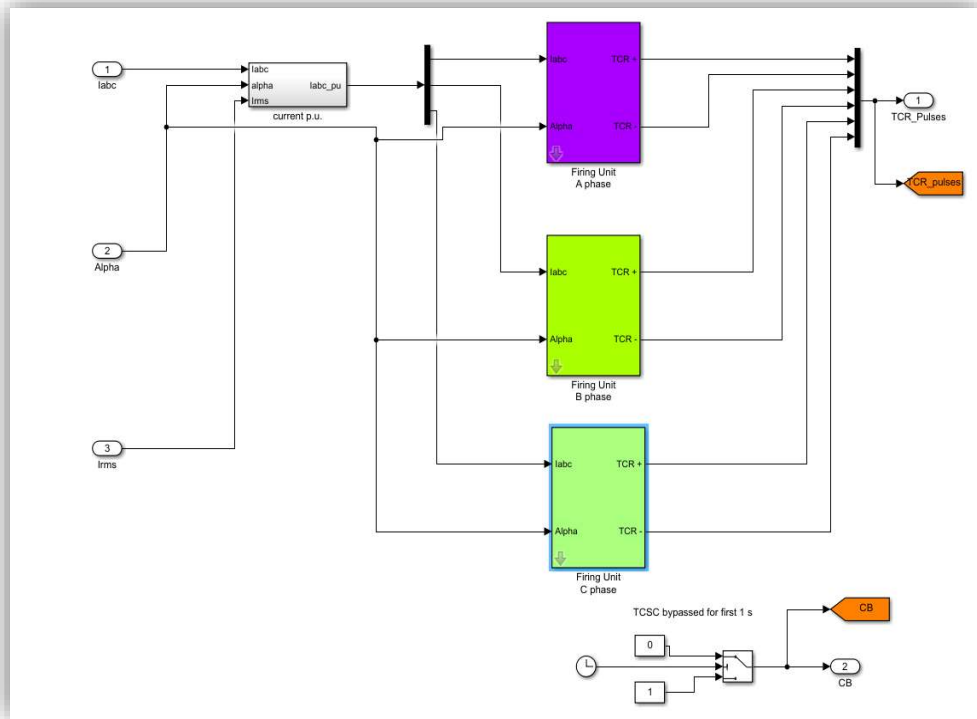


Figure 5-16 Simulink model of a firing unit

5.6 Simulation Results and Discussion

The proposed system's simulation results are tested on two different cases. The first involves placing TCSC at the sending end of the transmission line, while the second involves placing TCSC at the receiving end of the transmission line. The TCSC can work in either capacitive or inductive mode.

a. TCSC in Capacitive Mode of Operation

When the TCSC works in the capacitive mode of operation, TCSC's resonance is around 58 degrees of firing angle, and operation is prohibited between 49 and 69 degrees of firing angle. It should be noted that the overall system resonance is around 67 degrees. With firing angles ranging from 69 to 90 degrees, the capacitive mode is achieved.

Because the impedance is lowest at 90 degrees and highest at 69 degrees, power transfer increases as the impedance decreases. When the firing angle is 90 degrees, the maximum power is obtained, and when the firing angle is 69 degrees, the minimum

power is obtained. The impedance values in the capacitive mode operation range from 120 to 135 ohms. The simulation is carried out with an impedance value of 126 ohms.

Case 1: Installing TCSC with 70 % compensation at the transmission line-sending end.

a. Capacitive mode of operation

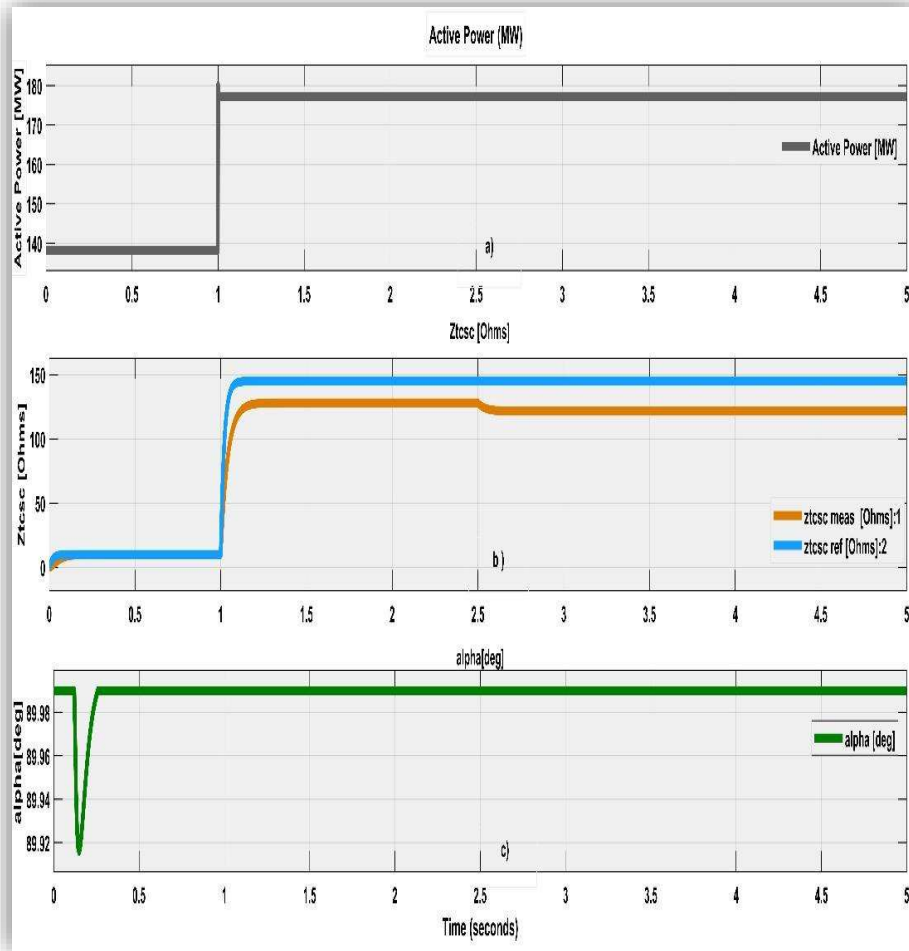


Figure 5-17 Sending end Active Power flow on the capacitive mode of operation

Figure 5-16 a) shows that the active power is increased by installing a TCSC at the sending end of a 230 kV transmission line. Without the TCSC, the power transfer is approximately 140 MW, based on the first 1 second of the simulation. The power transfer increases to 180 MW when the TCSC is inserted after 1 second with a 90-degree firing angle for the capacitive mode of operation. The transmission line's active

power increases by 28.5%. Figure 5-16 b) illustrates the system's maximum firing angle, which is 90 degrees. In addition, Figure 5-16 c) depicts the referenced and measured impedance values in the simulation. The impedance values in the capacitive mode operation range from 120 to 135 ohms. The simulation is carried out with an impedance value of 126 ohms.

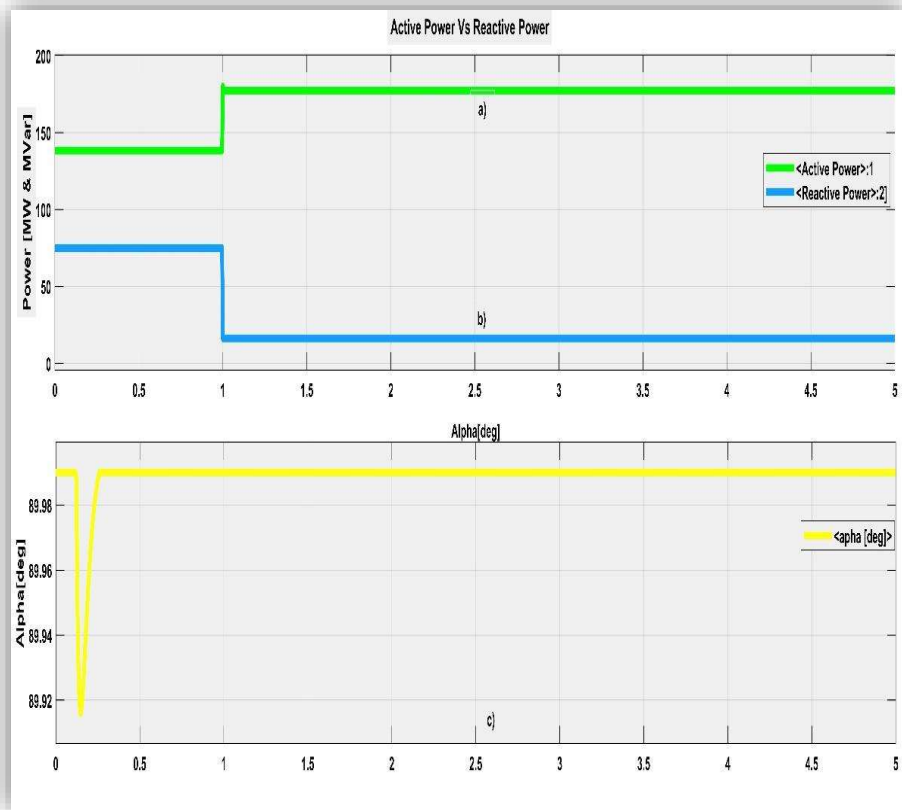


Figure 5-18 Sending end Active Power Vs Reactive Power on capacitive mode

The simulation result shown above illustrates the interaction of active and reactive power on a TCSC located at the transmission line's sending end. The simulation's first 1 second displays the system without TCSC. Figure 5-17 a) shows how installing a TCSC at the sending end of a 230 kV transmission line increases active power, and Figure 5-17 b) shows how the installation of a TCSC at the sending end of a 230 kV transmission line in capacitive mode reduces reactive power, and Figure 5-17 c) illustrates the system's maximum firing angle, which is 90 degrees.

Case 2: Installing TCSC with 70 percent compensation at the transmission line receiving end

a. Capacitive mode of operation

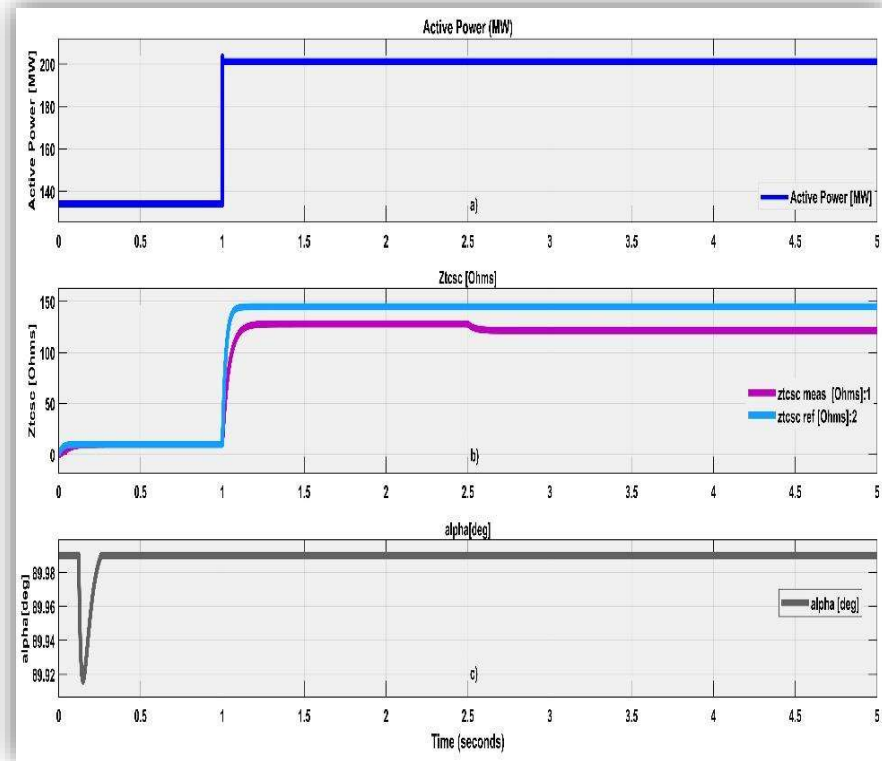


Figure 5-19 Receiving end Active Power flow on the capacitive mode of operation

Figure 5-20 a) shows how installing a TCSC at the receiving end of a 230 kV transmission line increases active power. Based on the first 1 second of the simulation, the power transfer without the TCSC is approximately 140 MW. When the TCSC is inserted after 1 second with a 90-degree firing angle for the capacitive mode of operation, the power transfer increases to 200 MW. The active power of the transmission line rises by 39%. Figure 5-20 b) depicts the system's maximum firing angle of 90 degrees. In addition, Figure 5-20 c) depicts the simulation's referenced and measured impedance values. In capacitive mode operation, the impedance values range from 120 to 135 ohms. The simulation is carried out with an impedance value of 126 ohms.

5.7 Cost-Benefit Analysis of TCSC

5.7.1 Cost of TCSC

TCSC has two main cost functions: the installation cost of TCSC devices in [US \$] and the cost of TCSC devices in [US \$/KVar].

The cost of installing TCSC devices has been mathematically calculated and is given by the following equation [41]–[44].

$$IC = C_{TCSC} \times S \times 1000 \quad (5-11)$$

Where

IC = the installation cost TCSC devices in [US \$]

C_{TCSC} = the cost of TCSC devices in [US\$/KVar]

The TCSC cost function is based on the Siemens AG Database, as shown below [42]–[44].

$$C_{tcsc} = 0.0015S^2 - 0.7130S + 153.7 \text{ [US\$/KVar]} \quad (5-12)$$

$$S = |Q_2 - Q_1| \quad (5-13)$$

Where:

Q_2 = Reactive power flow after TCSC installation

Q_1 = Reactive power flow before TCSC installation

S = Operation range of TCSC in [MVar]

a. TCSC at the Sending end of the transmission line cost.

Before the TCSC was installed, the reactive power was 74 MVar, and it increased to 82 MVar after the TCSC was installed on a transmission line.

$$S = |84 - 74| \text{MVar} \quad (5-14)$$

$$S = 8 \text{ MVar} \quad (5-15)$$

$$C_{tcsc} = 0.0015 \times 8^2 - 0.7130 \times 10 + 153.7 \text{ [US \$/KVar]} \quad (5-16)$$

$$\text{The total cost of the devices is } (C_{tcsc}) = 148.092 \text{ US \$/KVar} \quad (5-17)$$

$$\text{The total installation cost of TCSC} = C_{tcsc} \times S \times 1000 \quad (5-18)$$

$$IC = 148.092 \times 8 \times 1000 \quad (5-19)$$

Total installation cost = 1, 229, 594.292 US \$ or 63,938,903 ETB

b. TCSC at the Receiving end of the transmission line cost.

$$S = |84 - 74| \text{MVar} \quad (5-20)$$

$$S = 10 \text{ MVar} \quad (5-21)$$

$$C_{tcsc} = 0.0015 \times 10^2 - 0.7130 \times 10 + 153.7 [\text{US \$/KVar}] \quad (5-22)$$

$$\text{The total cost of the devices is } (C_{tcsc}) = 146.72 \text{ US \$/KVar} \quad (5-23)$$

$$\text{The total installation cost of TCSC} = C_{tcsc} \times S \times 1000 \quad (5-24)$$

$$IC = 146.72 \times 10 \times 1000 \quad (5-25)$$

IC = 1, 467, 200 US \$ or 76,294, 400 ETB

5.7.2 Benefit of TCSC

The revenue generated by the use of TCSC is calculated using the additional surplus and has a unit of “ US \$/ h ” or “ ETB / h ”.

When TCSC is installed at the transmission line's sending end, it increases active power flow by 40 MW, and also When TCSC is installed at the transmission line's receiving end, it increases active power flow by 60 MW.

a. Net annual surplus TCSC at the sending end

$$\text{Net annual surplus power/year} = P \times 8760 \quad (5-26)$$

$$= 40 \text{ MW} \times 8760 \quad (5-27)$$

Net annual surplus TCSC at the sending end = 350, 400 MWhrs

Appendix C contains the Ethiopian Electric Utility Generation Tariff. The generation Tariff Monthly Per KWH is 0.887.

$$\text{Net Annual Return} = 350,500 \text{ MWh} \times 0.887 \frac{\text{ETB}}{\text{KWh}}$$

$$\text{Net Annual Return} = 310,893,500 \text{ ETB}$$

b. Net annual surplus TCSC at the receiving end

$$\text{Net annual surplus power/year} = P \times 8760 \quad (5-28)$$

$$= 60 \text{ MW} \times 8760 \quad (5-29)$$

Net annual surplus TCSC at the receiving end = 525, 600 MWhrs

$$\text{Net Annual Return} = 525,600 \text{ MWh} \times 0.887 \frac{\text{ETB}}{\text{KWh}} \quad (5-30)$$

$$\text{Net Annual Return} = 466,207,200 \text{ ETB} \quad (5-31)$$

5.7.3 Payback Period

The payback period is the number of months of benefits required for the project to break even. The following equation can be used to calculate the payback time.

$$\text{Payback (Months)} = \frac{\text{Net Investment}}{\text{Net Annual Return}} \times 12 \quad (5-32)$$

Payback when TCSC is at the sending end

$$= \frac{63,938,903}{310,893,500} \times 12 = 2.46 \quad (5-33)$$

Payback when TCSC is at the receiving end

$$= \frac{76,294,400}{466,207,200} \times 12 = 1.963 \quad (5-34)$$

Many industrial companies prefer projects with a payback period of less than 1-2 years. Because of its life span, the net return of TCSC after 20 years of operation is zero.

CHAPTER SIX

6 CONCLUSION AND RECOMMENDATION

6.1 CONCLUSION

The inductive reactance of high voltage transmission lines frequently limits their power transfer capacity. In some cases, series compensation is used to reduce the transmission line's inductive reactance, thereby increasing the transmission line's power transfer capacity. A variety of methods have been developed to provide serial compensation for a transmission line. One of these methods is to use a thyristor-controlled series capacitor (TCSC).

A thyristor-controlled series capacitor is a type of flexible device used in alternating current transmission systems (FACTS). It is a variable capacitive and inductive reactance device for series compensation on high voltage transmission lines. The simulation of the Legetafo-Debre Birhan transmission line using the TCSC Controller was performed in this study. The degree of series compensation (K) is typically 30 to 70%, and in this paper, 70% of the line reactance is chosen for compensation.

A separate fuzzy logic controller is used in each operating mode to control the firing angle of the TCSC. Various test cases were done to validate the simulation's results. The first involves installing TCSC at the transmission line's sending end, and the second involves installing TCSC at the line's receiving end. The simulation is done in capacitive mode only due to the power factor is lagging.

When the TCSC is placed at the transmission line's sending end in capacitive mode, the active power flow increases from 140 MW to 180 MW, while the reactive power flow decreases from 74 MVAR to 20 MVAR. The total apparent power is 181 MVA. When the TCSC is placed at the receiving end of the transmission line in capacitive mode, the active power flow increases from 140 MW to 200 MW, while the reactive components fall from 74 MVAR to 10 MVAR, resulting in a total apparent power of 200.25 MVA.

The total cost, which includes the installation of TCSC at the sending end as well as the cost of the TCSC devices, is 63,938,903 ETB. After installation, the net annual return on the devices is 310,893,500 ETB. The devices have a payback period of 2.46 months, and the total cost, including the installation cost of TCSC at the receiving end and the

cost of the TCSC devices, is 76,294,400 ETB. After installation, the net annual return on the devices is 466,207,200 ETB. The devices have a payback period of 1.96 months, which is both economical and cost-effective.

Finally, the analysis concludes that installing TCSC at the receiving end of the transmission line is the most efficient and cost-effective method for increasing the power handling capacity for the case study area of the Legetafo to Debre Birhan transmission line.

6.2 RECOMMENDATION

- For EEP, the completed work can be expanded by installing TCSC on real-world networks.

6.3 Future work

- Checking the performance of TCSC by adding more TCSC to the system
- Considering the effect of TCSC, in the presence of other FACTS-type controllers.

REFERENCES

- [1] N. G. Hingorani and L. Gyugyi, *Understanding FACTS : concepts and technology of flexible AC transmission systems*. IEEE Press, 2000.
- [2] SERIES COMPENSATION BOOSTING TRANSMISSION CAPACITY - Google Scholar,” <http://www.abb.com/FACTS>.
https://scholar.google.com/scholar?hl=en&as_sdt=0%2C5&q=SERIES+COMPENSATION+BOOSTING+TRANSMISSION+CAPACITY+&btnG=
(accessed May 11, 2022).
- [3] A. Hassan, ... M. S.-W. T. on, and undefined 2013, “Power system quality improvement using flexible ac transmission systems based on adaptive neuro-fuzzy inference system,” *scholar.cu.edu.eg*, Accessed: May 11, 2022. [Online]. Available: http://scholar.cu.edu.eg/sites/default/files/mmustafa/files/3-m_ramadan1.pdf
- [4] “Enrique Acha, Claudio R. Fuerte-Esquivel, Hugo Ambriz-Pérez, César Angeles-Camacho - FACTS_ Modelling and Simulation in Power Networks- Wiley (2004)”.
- [5] Gebrmichael Gebre, “STUDY AND ANALYSIS OF THYRISTOR CONTROLLED SERIES CAPACITOR FOR IMPROVING OF TRANSMISSION SYSTEM CAPACITY (A Case Study on 500kV Dedesa Substation), Addis Abeba University,” 2017.
- [6] A. Yalew, “STUDY ON POWER TRANSFER CAPABILITY AND VOLTAGE STABILITY IMPROVEMENT USING STATIC VAR COMPENSATOR CASE STUDY: HOLETA 500 /400 kV SUBSTATION, Addis Abeba University,” 2019.
- [7] G. Zeleke, “LONG TERM LOAD FORECASTING AND TRANSMISSION SYSTEM EXPANSION PLANNING (CASE STUDY: CENTRAL AND SOUTHERN REGION OF ETHIOPIAN ELECTRIC POWER) ADDIS ABABA, ETHIOPIA,” Addis Abeba Universtiy, 2019.
- [8] M. R. S. Ananda M. H, “Effective Utilization of Transmission Line Capacity in a Meshed Network with Series Capacitor Upto its Thermal Limit,” *Int. J.*

Recent Technol. Eng., vol. 8, no. 6S, pp. 9–13, Mar. 2020, doi:
10.35940/ijrte.f1002.0386s20.

- [9] Institute of Electrical and Electronics Engineers, *2019 IEEE International Conference on Power, Intelligent Computing and Systems (ICPICS)*.
- [10] V. Golov, A. Kalutskov, and D. Kormilitsyn, “Controlled Series Compensation of High Voltage Lines to Increase Transmission Capacity,” *Proc. - 2020 Int. Ural Conf. Electr. Power Eng. Ural. 2020*, pp. 377–382, Sep. 2020.
- [11] N. Patel, “Hardware implementation and simulation of single phase TCSC at laboratory scale level,” N. Patel, “*Hardware Implement. Simul. single phase TCSC Lab. scale level*,” *2017 Int. Conf. Energy, Commun. Data Anal. Soft Comput. (ICECDS), 2017*, pp. 1755-1760.
- [12] P. Singh, R. Tiwari, V. Sangwan, and A. K. Gupta, “Optimal Allocation of Thyristor-Controlled Series Capacitor (TCSC) and Thyristor-Controlled Phase-Shifting Transformer (TCPST),” in *2020 International Conference on Power Electronics and IoT Applications in Renewable Energy and its Control, PARC 2020*, Feb. 2020, pp. 491–496.
- [13] C. Bulac *et al.*, “Power transfer capacity enhancement using SVC,” *2009 IEEE Bucharest PowerTech Innov. Ideas Towar. Electr. Grid Futur.*, pp. 1–5, 2009,
- [14] V. Komoni, I. Krasniqi, G. Kabashi, and A. Alidemaj, “Increase power transfer capability and controlling line power flow in power system installed the FACTS,” *IET Conf. Publ.*, vol. 2010, no. 572 CP, pp. 1–6, 2010.
- [15] S. Bagchi, R. Bhaduri, P. N. Das, and S. Banerjee, “Analysis of power transfer capability of a long transmission line using FACTS devices,” *2015 Int. Conf. Adv. Comput. Commun. Informatics, ICACCI 2015*, pp. 601–606, 2015.
- [16] R. Jena and S. C. Swain, “Comparative Analysis of STATCOM And TCSC FACTS Controller For Power,” no. Icces, pp. 407–413, 2017.
- [17] N. M. Malwar, S. R. Gaigowal, and A. A. Dutta, “Static Synchronous Series Compensator to enhance dynamic performance of Transmission Line,” *2016 Int. Conf. Comput. Power, Energy, Inf. Commun. ICCPEIC 2016*, pp. 743–746, 2016.

- [18] P. Nagar and S. C. Mittal, "Reactive power compensation by static synchronous series compensator," *Proc. - 2016 Int. Conf. Micro-Electronics Telecommun. Eng. ICMETE 2016*, pp. 301–304, 2016.
- [19] O. Ziaee and F. F. Choobineh, "Optimal Location-Allocation of TCSC Devices on a Transmission Network," *IEEE Trans. Power Syst.*, vol. 32, no. 1, pp. 94–102, 2017.
- [20] H. Putra and I. Joyokusumo, "An Analysis of Unified Power Flow Controller Placement Effect on Transmission Lines Total Transfer Capability," *2019 Int. Conf. Technol. Policies Electr. Power Energy, TPEPE 2019*, 2019.
- [21] A. A. Sallam and O. P. Malik, *Electric distribution systems*. 2018.
- [22] M. Lekshmi and K. N. Adithya Subramanya, "Short-term load forecasting of 400kV grid substation using R-tool and study of influence of ambient temperature on the forecasted load," *2019 2nd Int. Conf. Adv. Comput. Commun. Paradig. ICACCP 2019*, pp. 1–5, 2019.
- [23] H. Hahn, S. Meyer-Nieberg, and S. Pickl, "Electric load forecasting methods: Tools for decision making," *Eur. J. Oper. Res.*, vol. 199, no. 3, pp. 902–907, 2009.
- [24] Kevin Gurney, *AN INTRODUCTION TO NEURAL NETWORK*. UCL Press 1997.
- [25] K. L. Priddy and P. E. Keller, *Artificial Neural Networks: An Introduction*. 2009.
- [26] A. Ukil, *Intelligent Systems and Signal Processing in Power Engineering*. Springer-Verlag Berlin Heidelberg, 2007.
- [27] G. Montavon, "Introduction to Neural Networks," *Lect. Notes Phys.*, vol. 968, no. November, pp. 37–62, 2020.
- [28] M. Beale, M. Hagan, H. D.-T. MathWorks, and undefined 2010, "Neural network toolbox user's guide," *academia.edu*, Accessed: May 02, 2022.
- [29] X. P. Zhang, C. Rehtanz, and B. Pal, "Flexible AC Transmission Systems: Modelling and Control," *Power Syst.*, vol. 11, 2012.

- [30] J. V. Milanović, I. Papič, A. A. Alabduljabbar, and Y. Zhang, *Flexible AC transmission systems*, vol. 30. 2016.
- [31] R. M. Mathur and R. K. Varma, *Thyristor-based FACTS controllers for electrical transmission systems*. IEEE, 2002.
- [32] M. Venkatasubramanian and K. Tomsovic, *Power System Analysis*. 2005.
- [33] K. Manjusha, ... S. B.-... C. on P., and undefined 2016, “Real power flow control in transmission system using TCSC,” *ieeexplore.ieee.org*, Accessed: May 03, 2022.
- [34] B. Rigby, C. Ndlovu, R. H.-1999 I. A. 5th, and undefined 1999, “A thyristor controlled series capacitor design for research laboratory application,” *ieeexplore.ieee.org*, Accessed: May 03, 2022.
- [35] J. Paserba, N. Miller, ... E. L.-I. T. on, and undefined 1995, “A thyristor controlled series compensation model for power system stability analysis,” *ieeexplore.ieee.org*, Accessed: May 03, 2022.
- [36] Arthur R. Bergen Vijay Vittal, “Power System Analysis,” *Pearson Education Asia*, 2009.
https://scholar.google.com/scholar?hl=en&as_sdt=0%2C5&q=Arthur+R.+Bergen+Vijay+Vittal%2C+Power+System+Analysis&btnG= (accessed May 05, 2022).
- [37] S. Meikandasivam, R. K. Nema, and S. K. Jain, “Selection of TCSC parameters: Capacitor and inductor,” *India Int. Conf. Power Electron. IICPE 2010*, 2011.
- [38] D. Jovcic and G. N. Pillai, “Analytical modeling of TCSC dynamics,” *IEEE Trans. Power Deliv.*, vol. 20, no. 2 I, pp. 1097–1104, Apr. 2005.
- [39] Y. Bai and D. Wang, “Fundamentals of fuzzy logic control — fuzzy sets, fuzzy rules and defuzzifications,” *Adv. Ind. Control*, no. 9781846284687, pp. 17–36, 2006.
- [40] G. Chen and T. Tat Pham, “Introduction to Fuzzy Sets, Fuzzy Logic, and Fuzzy Control Systems Introduction to.”

- [41] S. A. Jumaat, I. Musirin, M. M. Othman, and H. Mokhlis, "Placement and sizing of thyristor controlled series compensator using PSO based technique for loss minimization," *2012 IEEE Int. Power Eng. Optim. Conf. PEOCO 2012 - Conf. Proc.*, pp. 285–290, 2012.
- [42] R. K. Suman, C. Lal, M. Kumar, I. Alam, and A. K. Goswami, "Cost-benefit analysis of TCSC installation to power system operation," *Proc. - 2011 Int. Conf. Energy, Autom. Signal, ICEAS - 2011*, pp. 635–640, 2011.
- [43] J. Kumar Muthukrishnan, S. S. Dash, H. Kiran Selvakumar, S. Chinnamuthu, and P. Panjamoorthy, "Comparison of optimization technique to find the optimal location of facts controllers for transmission line," *Am. J. Appl. Sci.*, vol. 11, no. 2, pp. 280–290, Dec. 2013.
- [44] A. K. Sharma, R. K. Mittapalli, and Y. Pal, "FACTS Devices Cost Recovery During Congestion Management in Deregulated Electricity Markets," *J. Inst. Eng. Ser. B*, vol. 97, no. 3, pp. 339–354, Sep. 2016.

APPENDIX

APPENDIX A: Matlab Code For Medium Transmission Line Parameter

```
clc
clear all
close all
L=input('Enter the length of the conductor:');
phase=input('Enter Phase:');
Pr = input('Receiving end Power: ');
Vr = input('Receiving end Voltage: ');
PF = input('Power Factor: ');
r = input('Resistance per Km: ');
x = input('Reactance Per Km: ');
Susceptance=input('The given value of susceptance:');
R = r*L;
X = x*L;
Z = R + j*X;
S=Susceptance*L;
Ic=j*S*Vr;
Method=input('Enter the desirable Method: \n 0-End Condenser Method \n 1-
Nominal-T \n 2-Nominal pi:\n');
if (Method==0);
    if(phase==1)
        I = Pr/(Vr*PF);
        I = I*(PF - j*sin(acos(PF)));
        Is=I+Ic;
        Vs = Vr + Is*Z;
        reg = (abs(Vs)-Vr)*100/Vr
        Ps = Pr+(abs(Is)^2*R);
        Efficiency = Pr*100/Ps
    elseif(phase==3)
        Vrph = Vr/sqrt(3);
        I = Pr/(3*Vrph*PF)
        I = I*(PF - j*sin(acos(PF)));
        Is=I+Ic;
        Vsph = Vrph + Is*Z;
        Vs = sqrt(3)*Vsph;
        reg = (abs(Vs)-Vr)*100/Vr
        Ps = Pr + 3*(abs(Is)^2)*R;
        Efficiency = Pr*100/Ps
    else
        disp('invalid phase');
    end
elseif (Method==1);
    if (phase==3)

        Vrph = Vr/sqrt(3);
```

```

I = Pr/(3*Vrph*PF);
I = I*(PF - j*sin(acos(PF)));
V1=Vrph+(I*(Z/2));
Ic=j*S*V1;
Is=I+Ic;
Vsph=V1+Is*(Z/2);
Vs=sqrt(3)*Vsph;;
reg = (abs(Vs)-Vr)*100/Vr
Losses=3*(abs(Is)^2)*(R/2)+3*(abs(I)^2)*(R/2);
Efficiency= ((Pr)/((Pr)+Losses))*100
elseif (phase==1)
I = Pr/(Vr*PF);
I = I*(PF - j*sin(acos(PF)));

V1=Vr+(I*(Z/2));
Ic=j*S*V1;
Is=I+Ic;
Vs=V1+Is*(Z/2);
reg = (abs(Vs)-Vr)*100/Vr
Losses=(abs(Is)^2)*(R/2)+(abs(I)^2)*(R/2);
Efficiency= ((Pr)/((Pr)+Losses))*100
else
disp('Invalid Phase');
end

elseif(Method==2)
if (phase==3)
Vrph = Vr/sqrt(3);
I = Pr/(3*Vrph*PF);
I = I*(PF - j*sin(acos(PF)));
Ic1=j*(S/2)*Vrph;
Il=I+Ic1;
Vs=Vrph+(Il*(Z));
Ic2=j*(S/2)*Vs;
Is=Il+Ic2;
reg = (abs(Vs)-Vr)*100/Vr
Losses=3*(abs(Is)^2)*(R/2)+3*(abs(I)^2)*(R/2);
Efficiency= ((Pr)/((Pr)+Losses))*100
elseif(phase==1)
I=Pr/(Vr*PF);
I = I*(PF - j*sin(acos(PF)));
Ic1=j*(S/2)*Vr;
Il=I+Ic1;
Vs=Vr+Il*Z;
Ic2=j*(S/2)*Vs;
Is=Ic2+Il;
reg = (abs(Vs)-Vr)*100/Vr
Losses=(abs(Is)^2)*(R/2)+(abs(I)^2)*(R/2);
Efficiency= ((Pr)/((Pr)+Losses))*100
end
end

```



```

for i = 1:ntotal
n = i - 1;
% year = first year + n
est_dem(i, 1) = past_dem(1, 1) + n;
% load growth equation
est_dem(i, 2) = Po*(1+g)^n;
if i <= np
fprintf('\t%4d\t%6.2f\t%6.2f\n', est_dem(i,1),past_dem(i,2),est_
dem(i,2));
else
fprintf('\t%4d\t\t\t%6.2f\n', est_dem(i,1),est_dem(i,2));
end
end
end
plot(past_dem(:,1),past_dem(:,2), 'k-s', est_dem(:,1), est_dem(:,2), 'k-+');
xlabel('Year'); ylabel('Demand'); legend('Actual', 'Forecast');

```

APPENDIX C: The Ethiopian Electric Utility Energy Tariff

Tariff Amendment	As of Dec.2018 onward	As of Dec. 2019 onward.	As of Dec. 2020 onward	As of Dec.2021 onward
Tariff Category	Birr/Kwh	Birr/Kwh	Birr/Kwh	Birr/Kwh
1. Bulk Supply Tariff				
1.1.Demand Charge rate per KW	39.2908	78.5815	117.8723	157.1600
1.2.Generation Tariff. Monthly per KWH	0.2218	0.4435	0.663	0.8870

APPENDIX D: Debre Birhan Substation Voltage Profile

Days	Urs Max(KV)	Urs Min(KV)	Urs Average(KV)
4/1/2021	237.37	227.18	232.93

4/2/2021	237.96	224.67	233.87
4/3/2021	237.86	225.40	233.72
4/4/2021	238.03	228.95	234.26
4/5/2021	237.59	227.03	234.22
4/6/2021	237.14	227.34	233.21
4/7/2021	238.56	208.59	233.62
4/8/2021	249.39	224.70	233.95
4/9/2021	238.10	227.14	233.33
4/10/2021	237.41	217.49	233.44
4/11/2021	238.15	227.84	233.87
4/12/2021	238.33	217.94	233.65
4/13/2021	251.30	0.00	197.54
4/14/2021	237.38	219.82	232.56
4/15/2021	237.04	228.31	232.65
4/16/2021	236.88	226.32	232.51
4/17/2021	237.90	222.16	232.45
4/18/2021	238.40	221.62	231.85
4/19/2021	237.34	221.06	232.99
4/20/2021	237.60	229.80	233.51
4/21/2021	237.78	221.11	232.87
4/22/2021	237.00	225.65	232.32
4/23/2021	236.25	222.63	232.71
4/24/2021	235.56	229.82	230.54
4/25/2021	237.04	227.42	233.67
4/26/2021	237.43	226.56	233.10

4/27/2021	237.48	226.57	233.10
4/28/2021	237.41	226.26	233.43
4/29/2021	236.41	227.44	233.45
4/30/2021	238.02	228.73	234.52

APPENDIX E: Debre Birhan Substation Receiving End Active Power (MW)

Days	Max Active P (MW)	Min Active P(MVar)	Average Active P(MW)
1/1/2021	118.34	0	47.24
1/2/2021	105.77	0.26	51.65
1/3/2021	110.6	0.5	52.54
1/4/2021	128.23	0.68	47.81
1/5/2021	108.6	0.62	55.66
1/6/2021	122.75	0.55	53.3
1/7/2021	97.98	1.4	56.72
1/8/2021	112.99	0.76	54.13
1/9/2021	122.75	1.75	60.08
1/10/2021	103.79	0	55.18
1/11/2021	117.41	0.29	53.31
1/12/2021	123.18	0.44	58.86
1/13/2021	108.71	0.06	50.84
1/14/2021	128.24	0.37	68.43
1/15/2021	105.65	0	56.49
1/16/2021	107.23	0.36	53.28

1/17/2021	98.53	0.33	60.59
1/18/2021	132.57	0	59.1
1/19/2021	102.78	1.68	63.19
1/20/2021	108.44	0.3	60.48
1/21/2021	112.49	3.33	71.12
1/22/2021	129.69	3.33	71.12
1/23/2021	118.42	0	63.36
1/24/2021	115.15	0.47	68.25
1/25/2021	134.42	0.62	68.02
1/26/2021	139.15	0.52	65.94
1/27/2021	138.97	5.03	72.16
1/28/2021	135.2	0.12	71.26
1/29/2021	108.25	3.19	73.94
1/30/2021	120.86	0.17	67.8
1/31/2021	107.61	0	67.21

APPENDIX F: Debre Birhan Substation Receiving End Reactive Power (MVAR)

Days	Max Reactive P(MVar)	Min Reactive P (MW)	Average Reactive P(MVar)
1/1/2021	49.99	22.22	38.24
1/2/2021	51.94	19.57	37.52
1/3/2021	51.49	16.95	40.89
1/4/2021	51.48	21.75	38.45
1/5/2021	51.59	22.28	36.43

1/6/2021	53.33	10.38	36.7
1/7/2021	54.5	3.71	36.47
1/8/2021	52.98	20.13	38.17
1/9/2021	75.16	18.94	40.38
1/10/2021	57.27	18.89	37.98
1/11/2021	53.11	21.06	36.42
1/12/2021	63.58	16.48	35.19
1/13/2021	56.54	18.64	38.04
1/14/2021	60.77	6	39.27
1/15/2021	53.53	23.45	39.52
1/16/2021	53.8	12.34	37.51
1/17/2021	54.29	14.76	35.5
1/18/2021	58.2	22.9	37.06
1/19/2021	63.34	4.03	35.45
1/20/2021	55.19	3.6	38.71
1/21/2021	59.59	18.55	38.79
1/22/2021	58.59	18.55	39.79
1/23/2021	56.84	6.75	36.11
1/24/2021	57.19	13.19	34.43
1/25/2021	62.61	8.15	37.11
1/26/2021	57.01	5.89	38.6
1/27/2021	72.75	17.62	39.7
1/28/2021	62.82	8.38	35.02
1/29/2021	65.18	20.8	40.46
1/30/2021	70.811	19.22	39.27

1/31/2021	63.31	24.61	41.38
-----------	-------	-------	-------

Appendix G: Debre Birhan Substation Receiving End Power Factor

Days	Max cos	Min cos	Average cos
1/1/2021	0.62	0.96	0.56
1/2/2021	0.89	0.95	0.43
1/3/2021	0.2	0.96	0.63
1/4/2021	0.52	0.96	0.57
1/5/2021	0.68	0.97	0.56
1/6/2021	0.8	0.99	0.51
1/7/2021	0.83	0.99	0.44
1/8/2021	0.67	0.96	0.56
1/9/2021	0.17	0.97	0.69
1/10/2021	0.55	0.97	0.58
1/11/2021	0.67	0.97	0.54
1/12/2021	0.9	0.99	0.43
1/13/2021	0.5	0.96	0.52
1/14/2021	0.42	0.99	0.64
1/15/2021	0.44	0.97	0.59
1/16/2021	0.88	0.97	0.52
1/17/2021	0.84	0.98	0.48
1/18/2021	0.63	0.98	0.57
1/19/2021	1	0.98	0.53
1/20/2021	0.51	0.98	0.6
1/21/2021	0.67	0.98	0.58

1/22/2021	0.67	0.98	0.58
1/23/2021	0.93	1	0.45
1/24/2021	0.66	0.98	0.6
1/25/2021	0.62	0.99	0.54
1/26/2021	0.33	0.99	0.61
1/27/2021	0.74	1	0.55
1/28/2021	0.77	0.99	0.51
1/29/2021	0.84	0.98	0.61
1/30/2021	0.69	0.98	0.62
1/31/2021	0.29	0.97	0.63